Photovoltaic Energy at South Pole Station

J. S. B. Mason

February 2007

Graduate Certificate in Antarctic Studies: ANTA504

Table of Contents

List of Figures

List of Tables

Acknowledgement

I would like to acknowledge the support of George Blaisdell, Operations Manager, U.S. Antarctic Program and Dr Alan Wood of the Electrical Power Engineering group at the University of Canterbury with this project,

I also appreciate the assistance of my colleagues at the University of Southampton, England namely Professor John Owen of the Department of Electrochemistry, who is my project supervisor for an on-going research project into modeling the performance of dye sensitised solar cells, and Dr Tomas Markvart of the School of Engineering Sciences for previous discussions on photovoltaic technology.

James S. B. Mason BSc(Hons) MBA CEng MIET SMIEEE
Christchurch, New Zealand
February 2007

Abstract

The energy requirements of Antarctic research bases are currently predominantly fulfilled by fuel oil which is used for heating and electrical generation. The cost of supplying this oil to Antarctica is high, both in economic and environmental terms. The amount of research that can be performed in the future is likely to become limited by the capacity to provide energy unless alternative solutions can be found. Recent events, such as the rise in fuel costs and the difficulty in ensuring reliable tanker deliveries provide strong economic and logistical pressures which promote alternative energy sources.

The USAP South Pole Station receives fuel oil indirectly through the McMurdo base, predominantly by air-supply, and consequently has a high energy cost. This research report will cover the opportunities for solar energy at South Pole Station, specifically photovoltaic technologies for electricity generation. Although there are clear disadvantages with solar power in the Antarctic, increases in energy demand coincide with the availability of solar resource. Consequently photovoltaic systems could provide a useful, supplementary power source for South Pole Station at relatively low cost.

Note

Costs are quoted in US dollars and fuel quantities are normally in US gallons.

1 US gallon = 3.785 litres

Introduction

The provision of energy is one of the most important issues currently confronting the global community as conventional fuel reserves are depleted; together with increased demand from developing countries and the environmental impact of burning fossil fuels. Consequently finding alternative energy sources and using conventional sources more efficiently are a clear priority for the worldwide community.

In Antarctica, the scientific bases are dependant upon imported fuel oil to maintain operations and to provide a safe working environment. The primary uses of the fuel oil is electricity generation, heating and transport (both ground and air operations). The cost of importing this fuel into Antarctica is high and so are the risks involved in its supply and distribution. Perhaps the greatest environmental threat to Antarctica from the operation of these bases is from oil pollution. The inaccessibility of Antarctica makes the cost of delivering fuel oil high, especially where bases are not accessible by sea. Consequently it would be highly desirable to reduce the dependence of Antarctic bases on fuel oil.

Sustainable energy sources, such as wind and solar power, provide an opportunity to provide alternative energy sources for Antarctica. Although the environment offers significant engineering challenges for the implementation of such systems, the high cost of present generation methods could make the implementation of renewable energy schemes attractive from an economic, as well as environmental, perspective.

Although solar energy is obviously limited in its application in Antarctica due to the months of darkness, it does offer advantages as a supplementary power source at permanent bases. Clearly base activity increases during the summer months and this leads to an increased demand for power. If solar energy could fulfill some of this demand then significant improvements in efficiency could be achieved. Although solar energy can be harnessed in various ways, for example in heating, water production and electrical generation, this report covers the application of photovoltaic[1] systems to generate electrical power in Antarctica.

South Pole Station provides a promising opportunity for the implementation of solar energy since it is at the end of a complicated and expensive logistics chain for the supply of fuel oil. The demands on the current system of logistical supply for fuel and generation capacity are creating pressures on the existing infrastructure which favour the provision of a supplementary power source.

[1] Also abbreviated to PV

South Pole Station

The Amundsen-Scott South Pole Station is a research station built by the United States at the Geographic South Pole. It is one of three year round stations operated by the NSF[2], the other two USAP[3] stations are McMurdo Station on the Ross Sea and Palmer Station on Anvers Island in the Antarctic Peninsular Region (Ref 1). The construction of South Pole Station originally started in November 1956 for the International Geophysical Year of 1957 and the station has been in continuous operation since that date. The base has been extended and relocated several times during this period with the construction of a new, elevated station beginning in 1999. The station location is at an elevation of 2835m and the recorded temperature has varied between -13.6°C and -82.8°C. These low temperatures, together with the low humidity and low air pressure at this altitude, can only be managed with proper protection at the base and survival is dependant upon the reliable and adequate supply of energy.

Figure 1: This aerial photo from October of 2005 shows the new South Pole Station in the upper right portion. The old station is the geodesic dome at the lower left

(from Scot Jackson, NSF)

[2] National Science Foundation
[3] United States Antarctic Program

The original station built in 1956-57 was eventually buried by wind blown snow which accumulates around the surrounding area of the building at a rate of about 1.3m per year. It was abandoned in 1975 and the station was relocated and rebuilt as a geodesic dome. The dome is 50m wide and 16m high and covers modular buildings, fuel storage bladders and other equipment. However the dome itself has also slowly been buried in snow drift. The new station building comprises of an adjustable elevation to avoid burial in snow and the facility is designed to be jacked up by one storey with the primary building columns being outhoard of the walls. The building also faces into the wind with a sloping lower section of wall which is designed to increase the wind speed as it is deflected under the building in an attempt to scour snow away from underneath the building.

The population of South Pole Station during the austral summer is around 250 with approximately 60 support staff and scientists wintering over. Between October and February, there are several flights per day of the ski-equipped LC-130 Hercules aircraft which supply the station. These aircraft also supply the fuel and the cargo carrying capacity of the LC-130 is a constraint. The limitations of this aircraft was cited by the NSF as one of the main reasons for the proposed development of an over-ice ground supply route (Ref 2).

The power plant at South Pole Station comprises of three Caterpillar 3512 diesel engines coupled to 750kW electrical generators with one Caterpillar 3412 and 250kW generator. The average electrical load at the base is around 620kW and one of the large generator sets operates continuously with another on standby, the smaller generator set is used for 'peaking' where intermittent loads increase the demand at certain times (Ref 3). This generation scheme provides a 'double firm contingency' model for operation[4] where one main generator set can be down for planned maintenance with one main operating and the other on standby. The power available at South Pole Station is limited to 750kW which can be achieved with a maximum output of 630kW from the main generator and 220kW from the peaking generator. Interestingly, the altitude of South Pole Station and the fuel type used result in a derating from the nominal maximum output of 750kW for the main generator sets. Thermal energy from the generator's water and jacket heat is also used for space heating of the primary station buildings. There is also an emergency power plant in a separate location which can be brought on line if the main power plant facility has a problem. The safety of the population at the base is dependant upon the reliable operation of this power plant.

Fuel Oil Specification

The majority of the fuel oil used at South Pole Station is AN8 which is used for generation, heating and turbine-powered aircraft with the remainder being other aviation and gasoline fuels, such as mogas for ground vehicles.

[4] Personal communication with G.L. Blaisdell, Operation Manager, USAP on 18-12-06

There are various grades of kerosine based fuels suitable for use in aircraft turbines, JP-8 is the military equivalent of Jet-A1 fuel used for commercial aircraft with the addition of corrosion inhibitor and anti-icing additives. The AN-8 fuel is a derivative of the JP-8 specification and is intended for Antarctic fuels operations, it must have a freeze point of minus 58°C or lower, while maintaining a flash point of 38°C or higher. Although specified for aircraft operations, the fuel is also compatible for operation in diesel powered electrical generation systems. The U.S. and New Zealand bases used Caterpillar power generation systems which have been modified to run on AN-8 fuel with recovery of the waste heat.

In the case of the bases located in the Ross Ice Shelf area and at the South Pole, the supply of AN-8 fuel is managed by the U.S. Antarctic Program with a yearly tanker delivery to McMurdo Sound. This shipment provides fuel for the U.S. McMurdo and South Pole stations, NZ Scott Base and the Italian Antarctic program. According to a recent tender document from the NSF[5] the nominal current annual requirements are:

Fuel (gallons)
- AN-8 3.5 million
- JP-5 3.0 million
- Gasoline 250 thousand

In May 2005, the NREL[6] estimated the cost of AN-8 fuel delivered to the South Pole to be between $12.00/gallon ($3.17/litre) and $15.70/gallon ($3.78/litre). It has been estimated that fuel which was being delivered to McMurdo in February 2007 for use during 2008 at South Pole Station will have cost about $20/gallon[7].

The Supply Chain

Delivery to McMurdo

The fuel oil is delivered to McMurdo Sound by a delivery tanker of the Military Sealift Command such as the 'Lawrence H. Gianella'. This vessel has a displacement of 39,624 tons and a reinforced bow which allows it to make fuel deliveries to Antarctica. In the tender document recently released by the NSF it states that:

'At present, fuel storage (ullage) in McMurdo is such that delivery of the above fuel quantities must be made each year. However, the USAP plans to increase the ullage such that skipping one year without re-fueling will be possible.

'Traditionally, the USAP has relied on the U.S. Coast Guard (USCG) to open a channel in the sea ice and then to escort cargo and fuel supply vessels using its POLAR class

[5] http://www.nsf.gov/about/contracting/dacs-usap-0107.htm
[6] National Renewable Energy Laboratory
[7] Personal communication with G.L. Blaisdell, Operations Manager, USAP on 14-12-06

ships. The cargo and fuel delivery vessels have been ice strengthened vessels chartered by the Military Sealift Command (MSC). The USCG vessels are 30 years old and are reaching the end of their design life. The MSC vessels are not configured for close coupling with icebreaking vessels configured with a towing notch.

'The U.S. Navy, Military Sealift Command provides these vessels for the USAP. The tanker loads at differing ports each year and arrives at the McMurdo ice edge on or about January 16. It departs on or about January 20 each year.

'Sea Ice
The fast ice in McMurdo Sound has typically been between 7 to 10 feet maximum thickness for a distance of 10 to 20 miles from McMurdo. It is often first or second year ice and had rarely been third year ice until very recently. For the past five years there have been extraordinary ice conditions due at least in part to the presence of large icebergs that were partially blocking McMurdo Sound. Ice thicknesses were as great as 12 feet. The icebergs have moved out of the area since last year. It is possible that the coming season's ice could start to return to a more normal status in the short term, but clearly conditions can change rapidly and persist for extended periods.'

Figure 2: The Lawrence H. Gianelli docking at McMurdo on 24th January 2001

(from http://groups.msn.com/Antarcticmemories/theoiltankerjan24)

The difficult sea ice conditions alluded to by the NSF were illustrated in 2001 when the Lawrence H. Gianella could not reach the dock at McMurdo after making several attempts using paths previously made by the Polar Sea icebreaker. Finally after pushing truck sized blocks of ice in front of its bow as shown in Figure 2, the ship made a final run towards the pier and reached a point which was close enough to haul hoses across the ice to allow the oil to be transferred.

The difficult sea ice conditions have been worsened by the prescence of the B-15A iceberg in the Ross Sea which has increased the icebreaking burden on the USCG Polar class icebreakers. There is serious concern that future iceberg movements could completely block access to McMurdo dock, the missing of one year's delivery of fuel or supplies would have serious implications for the operation of the US and New Zealand bases (page 8, ref 5)

Delivery to South Pole Station

South Pole Station is serviced and supplied from McMurdo Station by LC-130 aircraft from late October to February. The LC-130 Hercules, shown in Figure 3, is a four-engine turboprop transport aircraft which forms the backbone of U.S. transportation within Antarctica. The LC-130 is the polar version of the more familiar C-130 cargo plane. Its major unique feature is the ski-equipped landing gear which enables operation on snow or ice surfaces, it also has wheels for landings on prepared hard surfaces.

The aircraft has a cargo area of 12 by 3 by 3 meters and is used to carry fuel, cargo and personnel to South Pole Station. It can carry 12,200 kilograms of people and/or cargo from McMurdo to South Pole (728 nautical miles), then return to McMurdo without refueling and it cruises at 275 knots. The LC-130 can carry approximately 60% of its cargo payload as fuel and fuel can also be carried in wing tanks when the cargo load is less than the maximum load.

The NSF have stated that there were 333 LC-130 round trips to South Pole Station in 2005/06 (ref 6) which compares to around 130 flights in 1991 (ref 8). Although some of this increase has been due to the rebuilding of the station, the increased demand for fuel has also significantly increased flights. The NSF have six of these aircraft (with access to a seventh) and their availability is now becoming a bottleneck in the logistical support for South Pole Station. This has been recognized for some time and in a testimony before the House Committee on Science Subcommittee on Basic Research in 1999 (ref 9), Dr Karl Erb (Director of Polar Programs, NSF) stated that:

'Reducing flights to Pole. *Aircraft use about half the fuel delivered to McMurdo Station. Transport to South Pole, now done entirely by LC-130 flights from McMurdo, uses some two-thirds of each season's LC-130 missions (an LC-130 burns about 4,500 gallons of fuel to deliver 3,500 gallons to Pole). To maximize the load on each flight to Pole, fuel is carried in wing tanks to be delivered to the station when the cargo load is less than the weight the plane can carry. Still, LC-130 flights are one of our scarcest resources, and a*

priority is to minimize the Pole flights and free the precious LC-130s for missions such as open-field landings at remote antarctic research sites on snow or ice where there is no alternative.

'Several concepts are being analyzed. One is to use oversnow traverse vehicles-tractor trains-to resupply South Pole Station from a landing site closer to Pole than McMurdo is. Another would circle an Air Force KC-135 tanker over South Pole so that LC-130s equipped for air-to-air refueling could shuttle fuel down from the tanker to the station. A third idea is to build a hard-surface snow-ice runway at South Pole (comparable to the prepared Pegasus runway on glacier ice near McMurdo) so that wheeled airplanes can land with larger payloads, at lower cost per pound, than is possible with an LC-130 making a ski landing.'

Figure 3: A U.S. Air Force LC-130 Hercules carrying cargo for South Pole Station

(NSF photo http://www.nsf.gov/od/opp/support/lc130.jsp)

The South Pole traverse has demonstrated the feasibility of providing an alternative to LC-130 flights for delivering fuel as shown in Figure 4. A recent traverse has covered the full route and was described by the NSF[8] in a statement:

'The tracked vehicles staffed by a crew of seven men and one woman, towed sleds of cargo, fuel, and life-support modules left McMurdo on Nov. 11, 2005. During the 1028-mile (1654-kilometer) trip to the Pole, the tractor-train ascended more than 9,300 feet

[8] http://www.nsf.gov/news/news_summ.jsp?cntn_id=105718&org=NSF&from=news

(2,900 meters) and crossed numerous crevasse fields from sea level to the top of the Polar Plateau.

The convoy arrived at the South Pole on Dec. 23, 2005 (local time). U.S. stations in Antarctica keep New Zealand time.

In each of the past three years, traverses have covered steadily increasing distances between McMurdo and the Pole, encountering such difficulties as crevasse fields and enormous areas of soft snow that delayed their passage. This year the traverse reached its goal and delivered nearly 110 tons (99,790 kilograms) of cargo. The payload, which included two tractors, is equivalent to 11 loads of equipment and supplies aboard an LC-130'.

Figure 4: A tractor hooked up to fuel sleds waits to begin the South Pole Traverse.

(NSF/USAP photo by Kristan Hutchison, Raytheon Polar Services Corporation.)

The OAC Subcommittee on USAP Resupply (ref 10) has also recommended that the NSF seriously consider construction of a wheeled-aircraft-capable runway at the South Pole. This runway could alleviate several USAP resupply issues by allowing conventional aircraft to directly access the South Pole from McMurdo or other locations in Antarctica or off continent, for example New Zealand. Their findings suggest that results from previous snow mechanics studies could be used to develop a runway pavement design that would be capable of supporting the type of aircraft likely to operate at the South Pole such as the C-17 transport and KC-10 tanker aircraft.

Initiatives such as the South Pole traverse and the provision of improved runway facilities are unlikely to substantially reduce the fuel cost at South Pole Station but are intended to improve the capacity and reliability of the logistical supply chain.

Energy Costs at South Pole Station

The high cost of energy at South Pole Station is reflected in the cost of importing fuel oil by air tanker, in their 2005 report (ref 10) the OAC estimated:

'The cost of one liter of fuel delivered to South Pole Station is about $6.58 ($25/gal), or $17,500,000 for 2,660,000 liters, using the traditional McMurdo resupply route. This considers the initial cost of the fuel, the prorated charter cost of the tanker vessel, the prorated cost of the icebreaker(s), and the prorated flight hour costs and number of LC-130 missions flown to South Pole (320 in 2004/2005 season, of which 60% of the payload moved was fuel).'

In the earlier section Fuel Oil Specification, it was seen that the NREL estimated the cost of AN-8 fuel delivered to the South Pole in 2005 to be between $12.00/gallon ($3.17/litre) and $15.70/gallon ($3.78/litre). Consequently, taking into account fuel prices increases since these estimates, **a conservative estimate of AN-8 fuel delivered at South Pole Station would be $20/gallon in 2007 v**alues.

A South Pole fuel usage spreadsheet for July 2005 to July 2006 (ref 11) shows that 377,421 gallons out of a total of 783,682 gallons of fuel at South Pole Station was used for power generation with the total fuel usage breakdown shown in Figure 5.

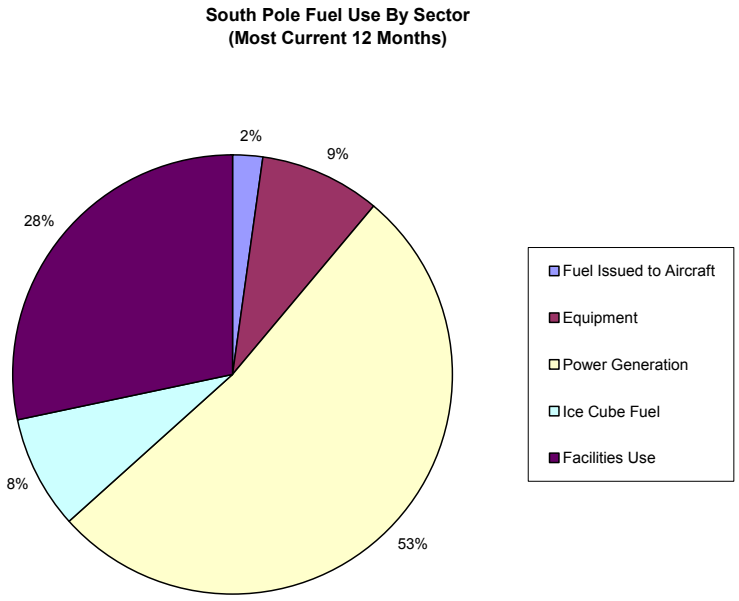

Figure 5: Fuel usage at South Pole Station, July05-July06

(from SouthPoleFuelUseage-July05-July06 at http://astro.uchicago.edu/scoara/2006-power/index.htm)

The average power generation at South Pole Station is 620kW averaged over the year and this correlates with the fuel consumption as shown in Figure 6.

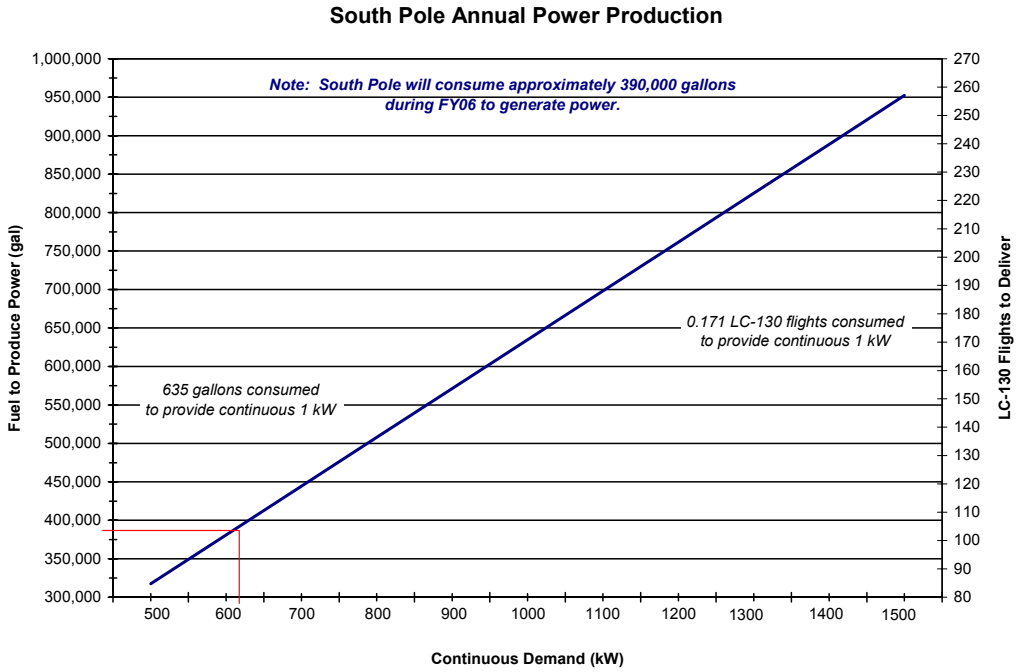

Figure 6: South Pole annual fuel consumption vs generated electrical power

(from kW-gal-graphrsa.xlx at http://astro.uchicago.edu/scoara/2006-power/index.html)

The fuel required to generate a continuous kW of electricity is 377421/620 = 608 gallons, the spreadsheet calculation shown in Figure 6 is slightly higher at 635 gallons as the annual fuel consumption is approximated to a higher value.

A LC-130 aircraft consumes 4778 gallons for the round trip to the South Pole (burn rate 735 gallons/hour and 6.5 hour flight duration) with a fuel payload of approximately 3700 gallons. Hence to produce a continous kW of power requires 635/3700 = 0.171 LC-130 flights.

A standard measure of electrical energy is the kWh which is the amount of energy required to deliver 1kW of power for 1 hour. At South Pole Station, the generators are providing an average power of 620kW with an hourly fuel consumption of 377421/(365*24) = 43.08 gallons which equates to a cost of 43.08*20 = $861. Therefore the fuel cost per kWh of electricity is 861/620 = $1.39.

Of course this is not the full cost of electrical generation at South Pole Station, this would need to include the depreciation costs of the Caterpillar generation sets and the associated infrastructure and support which are considerable. However it does indicate

the savings that could be made if some of the electrical demand could be provided by other generation methods which supplemented the diesel generators.

In comparison, the average commercial electricity charge in Christchurch, New Zealand for 2007 is around 15 NZcents/kWh or $0.10/kWh.

Any load removed from the diesel generators by, for example by a renewable energy scheme, will be seen as a fuel saving. In a Scott Base Energy Audit (ref 12), it was reported that:

'Any renewable energy scheme will save electricity – each average kilowatt saves 2400 litres of fuel per year. Further studies are required for renewable source/diesel generator interactions.'

This converts to a saving of 634 US gallons.

The main power generation capacity at Scott Base is provided by two diesel electric Caterpillar 3604 generators (up to 200kW electrical load) with one running and the other on constant standby. An average load of 1kW on each generator uses about 6.5 litres of fuel per day which equates to 2400 litres or 634 gallons per year.

This correlates well with the South Pole Station generators which are slightly more efficient (with an average load of 1 kW consuming 608 gallons annually) probably due to their greater capacity and some previous engineering development on the system to improve efficiency through supercharging and cooling of the air inlet.

Consequently, the conclusions from the Scott Base Energy Audit should be applicable to the South Pole Station situation with any load removed from the diesel generation system being seen as a direct fuel saving. This study also alludes to the issue of renewable source/diesel generator interactions. In the case where only part of the electrical load is being replaced by an alternative source then some consideration needs to be given to how the energy is supplied into the system and this will be covered later in the report.

The Potential for Renewable Energy

The most commonly applied renewable energy technologies are wind and solar and both have been applied in Antarctic in various schemes. Solar energy is commonly employed in two forms, either solar heating, normally for space or water heating, or photovoltaic technology which provides direct generation of electricity from light. Although all of these technologies have possible application at South Pole Station, this report is specifically concerned with the application of photovoltaic technology.

Meteorological and Solar Data for South Pole Station

NASA[9] provides surface meteorology and solar energy (SSE) data derived from satellites for any location defined by latitude and longitude (ref 13). This SSE data is a continuous and consistent 10-year global climatology of insolation[10] and meteorology data on a 1° by 1° grid system. This data is considered to be the average over the entire area of the cell and is not necessarily representative of a particular microclimate, or point, within the cell, however this is unlikely to be an issue in the South Pole application. This resource provides a useful basis for assessing the feasibility of solar energy schemes.

The following results are for the South Pole:

Monthly Averaged Insolation Incident On A Horizontal Surface (kWh/m^2/day)													
Lat -90 Lon 0	Jan	Feb	Mar	Apr	May	Jun	Jul	Aug	Sep	Oct	Nov	Dec	Annual Average
10-year Average	8.64	4.67	0.46	0.00	0.00	0.00	0.00	0.00	0.09	2.96	7.34	9.64	2.81

(Insolation is the measure of solar radiation energy incident on a surface; its value above the earth's atmosphere, also called the solar constant, is close to 1.367 kWh/m^2)

Monthly Averaged Cloud Amount At Indicated GMT Times (%)												
Lat -90 Lon 0	Jan	Feb	Mar	Apr	May	Jun	Jul	Aug	Sep	Oct	Nov	Dec
Average@0	8.33	16.3	n/a	n/a	n/a	n/a	n/a	n/a	n/a	n/a	14.1	5.80
Average@3	9.92	16.9	n/a	n/a	n/a	n/a	n/a	n/a	n/a	n/a	13.8	5.54
Average@6	11.1	14.5	n/a	n/a	n/a	n/a	n/a	n/a	n/a	n/a	9.19	4.29
Average@9	6.38	17.6	n/a	n/a	n/a	n/a	n/a	n/a	n/a	n/a	11.8	5.09
Average@12	6.55	18.1	n/a	n/a	n/a	n/a	n/a	n/a	n/a	n/a	12.7	4.30
Average@15	5.45	17.0	n/a	n/a	n/a	n/a	n/a	n/a	n/a	n/a	10.9	5.21
Average@18	6.74	15.8	n/a	n/a	n/a	n/a	n/a	n/a	n/a	n/a	11.2	4.97
Average@21	7.49	16.9	n/a	n/a	n/a	n/a	n/a	n/a	n/a	n/a	15.1	6.34

Monthly Averaged Wind Speed At 50 m Above The Surface Of The Earth (m/s)													
Lat -90 Lon 0	Jan	Feb	Mar	Apr	May	Jun	Jul	Aug	Sep	Oct	Nov	Dec	Annual Average
10-year Average	4.63	5.59	7.02	7.33	7.35	7.13	7.16	7.25	7.24	6.30	4.91	4.15	6.34

[9] National Aeronautics and Space Administration
[10] **In**cident **sol**ar radi**ation**

Minimum And Maximum Difference From Monthly Averaged Wind Speed At 50 m (%)													
Lat -90 Lon 0	Jan	Feb	Mar	Apr	May	Jun	Jul	Aug	Sep	Oct	Nov	Dec	Annual Average
Minimum	-8	-10	-11	-8	-7	-6	-4	-5	-6	-5	-11	-17	-8
Maximum	8	9	5	5	5	6	7	2	7	5	13	19	8

Monthly Averaged Air Temperature At 10 m Above The Surface Of The Earth For Indicated GMT Times (° C)												
Lat -90 Lon 0	Jan	Feb	Mar	Apr	May	Jun	Jul	Aug	Sep	Oct	Nov	Dec
Average@2230	-21.4	-29.7	-46.8	-55.9	-58.1	-59.3	-61.3	-64.1	-63.2	-52.1	-30.1	-21.4
Average@0130	-21.5	-29.9	-47.2	-55.9	-58.1	-59.3	-61.3	-64.0	-63.2	-52.2	-30.1	-21.4
Average@0430	-21.6	-30.1	-47.7	-55.9	-58.1	-59.4	-61.3	-64.0	-63.2	-52.4	-30.2	-21.5
Average@0730	-21.7	-30.2	-47.7	-56.0	-58.1	-59.5	-61.3	-63.9	-63.2	-52.3	-30.2	-21.5
Average@1030	-21.6	-30.2	-47.8	-56.1	-58.2	-59.5	-61.3	-63.9	-63.2	-52.0	-30.0	-21.5
Average@1330	-21.6	-30.1	-47.6	-56.3	-58.2	-59.5	-61.4	-63.9	-63.2	-51.7	-29.7	-21.3
Average@1630	-21.5	-30.0	-47.2	-56.2	-58.2	-59.5	-61.4	-63.9	-63.1	-51.4	-29.6	-21.3
Average@1930	-21.5	-30.0	-47.0	-56.1	-58.2	-59.4	-61.5	-63.9	-63.1	-51.4	-29.6	-21.2

This data suggests that the South Pole is a reasonable solar site during the months of daylight with high levels of insolation and relatively low cloud cover. The efficiency of photovoltaic cells generally increases with reducing temperature, the coefficient of the maximum power with temperature for a silicon cell is around -0.4%/°C. Consequently, a significant increase in rated power can be achieved in this environment. The relatively low wind speeds also suggest that wind loading effects on PV array structures will not be a problem.

A Comparison with Leading Solar Sites

It is useful to compare the insolation available at the South Pole with two other sites where PV technology is being applied on a large scale. Serpa in Portugal is one of Europe's sunniest areas and in April 2006, GE Financial Services, Powerlight Corporation and Catavento Lda announced that this was to be the location of a 11MW solar power plant incorporating 52,000 PV modules. NREL researchers have rated the San Luis Valley in south-central Colorado, USA as having the state's best solar exposure. An 8MW solar power plant is planned for this location by Xcel Energy to be online by the end of 2007. The SSE data has been obtained for these two locations and then plotted against the South Pole data as shown in Figure 7.

Serpa, Portugal

Monthly Averaged Insolation Incident On A Horizontal Surface (kWh/m^2/day)													
Lat 37.933 Lon -7.583	Jan	Feb	Mar	Apr	May	Jun	Jul	Aug	Sep	Oct	Nov	Dec	Annual Average
10-year Average	2.31	3.00	4.36	5.20	6.15	6.88	7.34	6.50	5.21	3.51	2.41	1.94	4.57

San Luis Valley, Colorado

Monthly Averaged Insolation Incident On A Horizontal Surface (kWh/m^2/day)													
Lat 37.433 Lon -105.85	Jan	Feb	Mar	Apr	May	Jun	Jul	Aug	Sep	Oct	Nov	Dec	Annual Average
10-year Average	2.35	3.26	4.41	5.52	6.40	6.55	6.03	5.39	4.80	3.81	2.73	2.18	4.45

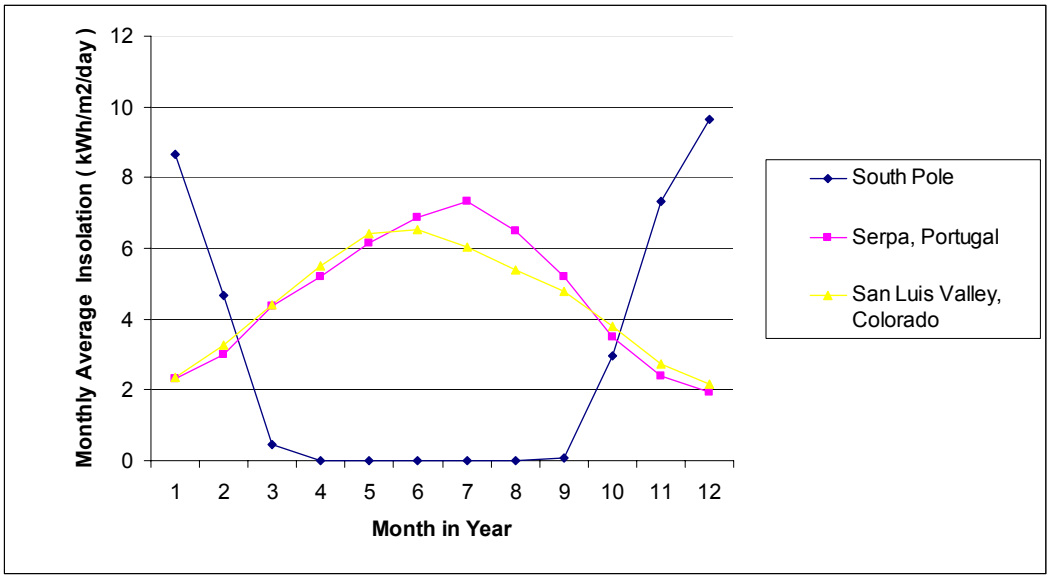

Figure 7: Average insolation vs month for the South Pole, Serpa (Portugal) and the San Luis Valley (Colorado, USA)

(from NASA SSE website data)

These results show the high values of insolation achieved at the South Pole during summer which, together with the low operating temperature, will result in high relative outputs from a PV installation. Averaged over the year, the South Pole could still achieve 60% of the output produced at some of the world's best solar locations.

The Cost of Photovoltaic Technology

Although the cost of a photovoltaic installation is dependant upon many factors, such as the technology deployed and location, it is possible to make some broad estimates of costs based on installed power capacity. The cost per unit of energy produced can also be estimated from calculations of the energy produced by the PV system over its lifetime and the depreciation of the system cost over this period. In commercial applications, PV systems are expected to last for at least twenty years and many manufacturers now certify their products with 20 or 25 year guarantees on their electrical output under standard conditions. Substantial operational experience has been obtained with the silicon PV technologies which allow their performance and costs to be accurately specified.

In 2002, the National Renewable Energy Laboratory produced an energy cost trend[11] for photovoltaic generation showing the levelised cents/kWh, with the cost corrected to the year 2000 value, and this is shown below in Figure 8**.**

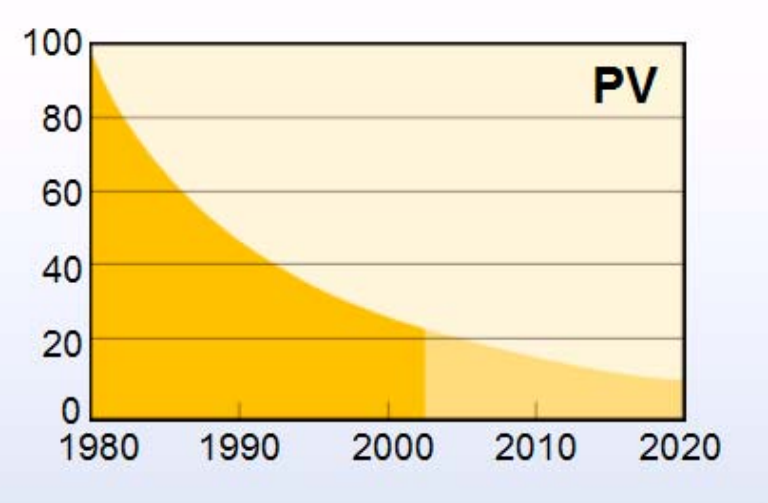

Figure 8: Energy cost trend for PV systems- 2000 cost in cents per kWh vs year

In September 2006, Gary Schmitz, a spokesman for the NREL commented[12] that solar power from photovoltaic panels currently costs about 22 cents to 25 cents per kWh but he expected "the cost to come down substantially in the next 10 years".

In the Antarctic application, these costs will be higher due to the increased costs of transportation and installation of the system, together with the absence of solar resource during the austral winter. However, the high cost of current electricity generation, estimated at $1.39/kWh in Energy Costs at South Pole Station, suggests that there could

[11] NREL Energy Analysis Office (www.nrel.gov/analysis/docs/cost_curves_2002.ppt)
[12] SunEdison to build solar farm (RockyMountainNews.com September 23, 2006)

be potential for photovoltaics based on an economic justification. Clearly there would be other good reasons, such as environmental, to also consider their application.

An Overview of Commercial Photovoltaic Technologies

A detailed description of the operation of photovoltaic devices is beyond the scope of this report and can be found in the cited references. However, a brief description of the evolution of the technology and basic device operation is provided since it does provide a useful background to the selection of the appropriate technology for this application.

A Brief History

The photovoltaic effect was first reported by Bequerel in 1839 after he observed an electric current when light illuminated a silver coated platinum electrode immersed in an electrolyte. The first solid state photovoltaic device was constructed in 1876 when Adams and Day noticed that a photocurrent could be produced in selenium. Although selenium can also be used to make photoconductive devices, where the resistance of the device changes with illumination, in this case a photovoltaic device had been produced where current was produced from light. This was due to a rectifying junction formed between the selenium material and platinum contacts. At the time, the underlying theory behind the operation of these devices was not understood. It was not until the 1930s when the theory of metal-semiconductor devices was developed by researchers such as Schottky and Mott that the physics of the selenium cell began to be understood. These devices, although not practical for power generation, did find application in areas such as photographic light meters.

In 1904, Einstein published his paper on the photoelectric effect along with his theories on relativity. In 1916, Millikan provided experimental proof of the photoelectric effect and in 1921, Einstein received the Nobel prize for this work.

In the late 1940s, the revolutionary research in the U.S. at the Bell Laboratories into semicnductor physics, which lead to the invention of the transistor in 1947, developed the underlying theory behind semiconductor diode junctions. In the early 1950s, Ohl had found that sunlight incident on silicon produced an unexpectedly high current to flow. The first silicon solar cell was reported by Chapin, Fuller and Pearson of Bell Laboratories in 1954 and their reported conversion efficiency of electricity from sunlight at 6% was around six times better than the previous best device. An early solar demonstration is shown in Figure 9 and this lead to a New York Times article predicting that this invention could eventually lead "to the realization of one of mankind's most cherished dreams -- the harnessing of the almost limitless energy of the sun."

In 1953, Trivich made the first theoretical calculations of the efficiencies of various materials which could be used for constructing solar cells based on their band gap values

and the energy spectrum from the sun. Consequently, it was known that the efficiency could be significantly improved from 6% but with an estimated production cost of $200 per Watt of electricity, this technology was not seriously considered for terrestrial power generation for several decades. However the emergence of the space industry in the 1950s and 1960s, where the requirements of reliability and low weight were more significant than cost, promoted the development of solar cell technology. Since 1954, devices have been built from a range of materials where theoretical work has indicated higher efficiencies or better performance in other parameters such as cost. However, silicon still remains the foremost photovoltaic material benefiting from the enormous knowledge and investment in silicon by the wider microelectronics industry.

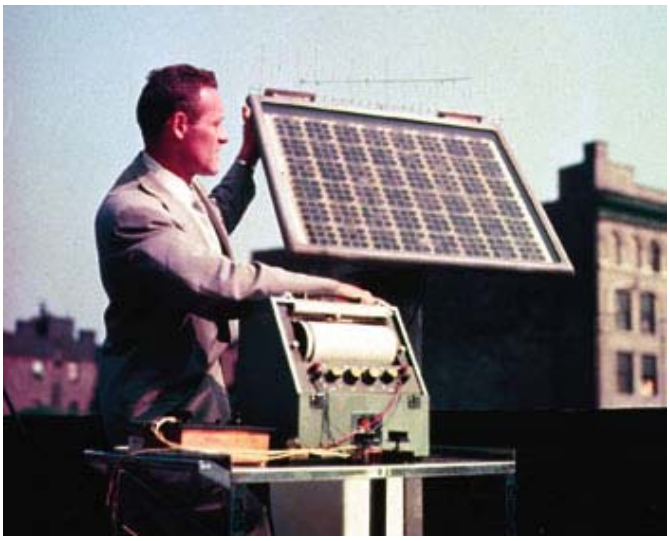

Figure 9: A Bell Labs engineer testing a solar battery in 1954

(from Bell Labs website)

Device Operation

The semiconductor p-n junction forms the basis of the silicon solar cell. A semiconductor is a material which has an electrical conductivity between insulators and metals. In the case of silicon, the intrinsic material (the pure state where it is undoped) has an electrical resistivity of around 2500Ωm and the concentration of impurity atoms is less than 1 in 10^9. The cost of processing silicon to reach these required levels of purity is high and this is a limiting factor of the technology.

The electrons of the silicon atoms which form the crystalline structure of the semiconductor can be considered within the framework of an energy band model with each energy band being able to take a limited number of electrons. The highest fully occupied band is called the valence band and is responsible for bonding atoms together within the crystal. Since silicon is in Group IV of the periodic table, it has four valence electrons and so bonds with four other silicon atoms in the crystal lattice. The valence band is separated from the next highest band, called the conduction band, by the **band gap**. The occupation of the conduction band by electrons determines whether a material

is a conductor or an insulator. In semiconductors, the band gap is lower than for insulators and electrons can receive energy from light stimuli causing them to move from the valence to conduction bands. The electron leaves behind a vacancy in the valence band and the 'hole' formed represents a charge carrier of opposite polarity to the electron. When electrons are excited into the band gap they become mobile electrons and can travel through the crystal lattice, with holes effectively moving in the opposite direction. Consequently, the conductivity of the material increases conversely reducing its resistivity. This effect is known as photoconductivity and is the phenomenon which was first observed and made researchers aware of photovoltaic materials.

The electrical properties of a semiconductor can be modified by adding so-called dopant materials. If impurity atoms with a higher valency, for example antimony from Group V, are added to the crystal lattice then they have one too many valence electrons for the number of crystal bonds. These impurities donate an extra electron to the crystal lattice and are therefore called donor atoms. This extra electron is bound less well than the other four electrons to the antimony atom and can relatively easily leave the atom and become a charge carrier within the crystal lattice, thereby leaving behind a fixed positively charged antimony ion. In this case, the electron density is now increased over its equilibrium value, corresponding to the undoped or intrinsic state, and the hole density is reduced. Consequently, the electrons are termed majority carriers and the holes the minority carriers in this material. A semiconductor which has been doped in this way to increase the density of electrons relative to holes is termed n type and is extrinsic.

Conversely if impurity atoms with a lower valency, for example boron from Group III, are added then they have too few valence electrons for the number of crystal bonds. This acceptor atom now becomes ionized releasing a hole into the valence band. A p type semiconductor is then formed with an excess of holes which are positive carriers. Again the conductivity of the material is greatly increased compared to its intrinsic state but now the majority carriers are holes. The action of the doping process described is shown in Figure 10.

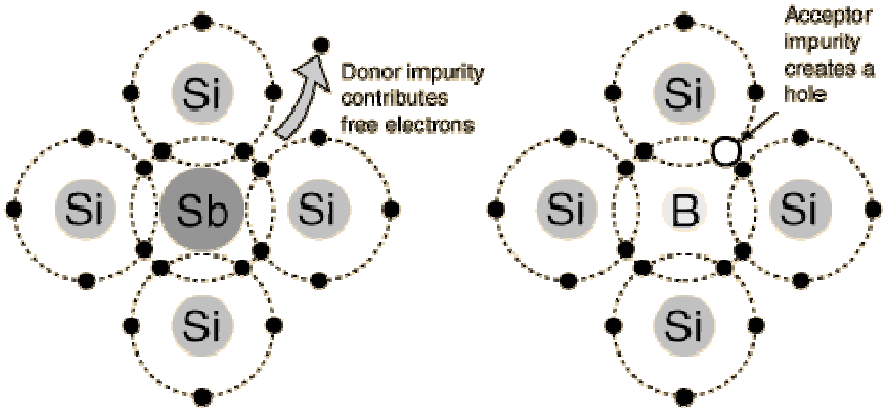

Figure 10: Creating n and p type semiconductors using doping of antimony (Sb) and boron (B) atoms

(from http://hyperphysics.phy-astr.gsu.edu/hbase/solids/dope.html#c3)

The basis of most commercial photovoltaic devices is the semiconductor junction, most commonly a p-n junction which is formed by joining p-type and n-type semiconductor materials. When p and n type regions meet at a junction, the majority carrier electrons from the n region cross over the junction to the p region and vice-versa for the holes. At the junction boundary, a depletion region (also referred to as a space charge region) is formed. This has few free carriers but contains the fixed ions of the dopant atoms left behind in the respective material as shown in Figure 11.

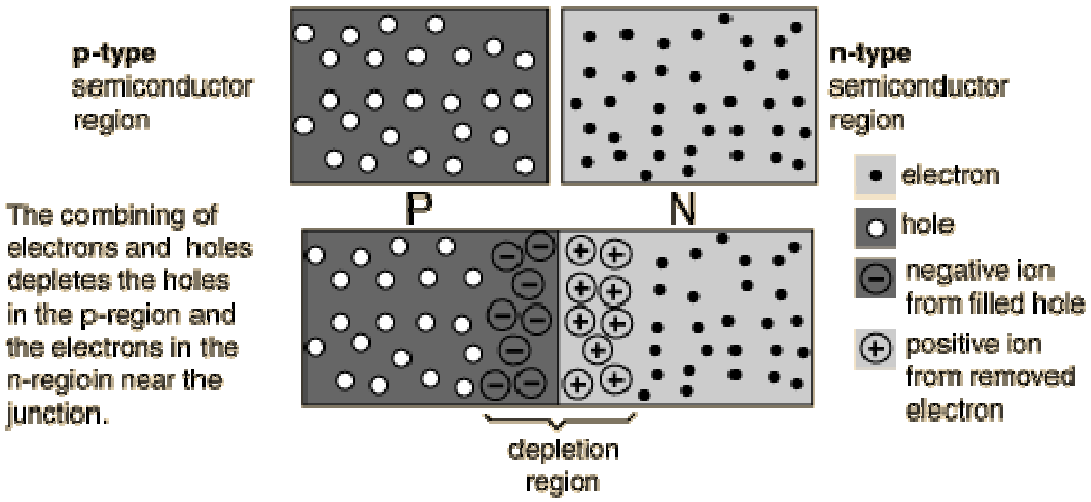

Figure 11: Formation of the depletion region in a semiconductor P-N junction

(from http://hyperphysics.phy-astr.gsu.edu/hbase/solids/pnjun.html#c1)

The charge associated with these ions forms a counteracting electric field. The flow of carriers occurs until equilibrium is reached where the electric field, caused by the accumulation of charge on each side of the junction, balances the diffusion resulting from the different concentrations of free electrons and holes. This electric field establishes a voltage across the junction which is around 0.5V for silicon. It is this electric field which allows light generated carriers to be separated out to the respective electrodes of the photovoltaic cell which connect to the p and n regions.

The photoelectric effect is responsible for generating electrons within the semiconductor p-n junction. In 1905, Einstein explained that light could be considered in terms of a wave and particle duality with the particles, called photons, having an energy which was proportional to their frequency. Light is a form of electromagnetic radiation with the visible band ranging in frequency from around 4.3×10^{14} - 7.5×10^{14} Hz. On hitting an electron, the photon can transfer its energy to the electron and if this is enough energy then in the case of a semiconductor, the electron is excited from the valence to the conduction band. The energy required for the transfer of an electron between these bands is given by the bandgap of the material. If the photon does not have enough energy to excite the electron into the conduction band then the photon is not absorbed. When the

photon has more than the energy required then the electron is excited into the conduction band and the excess energy is lost as heat. Consequently, the bandgap of the semiconductor material is important for determining how much of the incoming light energy is converted into electricity within a photovoltaic device.

In a photovoltaic device, energy conversion results when:

1. The incoming light energy generates charge (exciting an electron from the valence to conduction band)
2. The charge can be separated (using the field of a p-n junction)
3. The charge can be transported (using carrier flow within the semiconductor and electron flow through the external circuit)

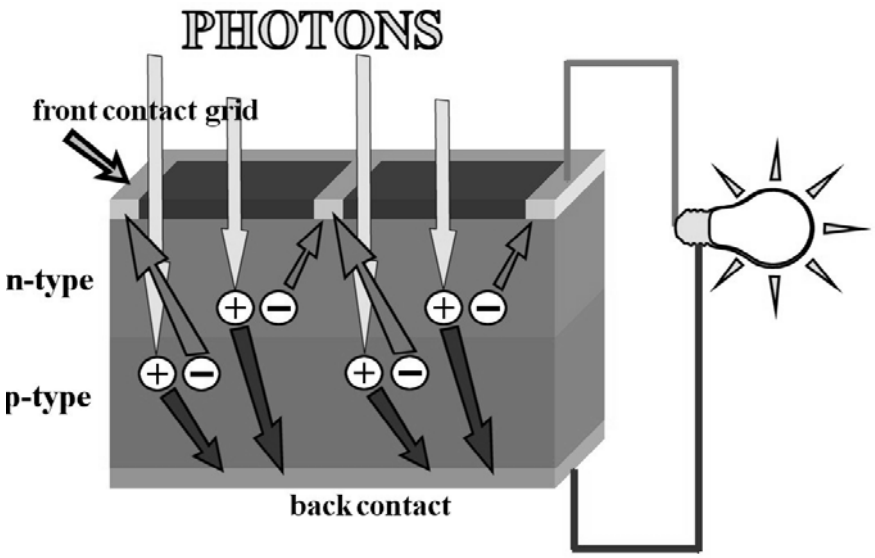

Figure 12: Current generation and flow in a PV cell

(from http://www.specmat.com)

This operation is illustrated in Figure 12, incoming photons enter the crystal lattice of the p-n junction photovoltaic cell and excite electrons into the conduction band. The inherent field associated with the p-n junction pull the electrons to the contact of the n-type semiconductor and the associated holes are attracted to the contact of the p-type semiconductor. Connecting an electrical load between the contacts of the cell provides a path for the electrons to flow and to recombine with the holes, in so doing they are performing work and delivering energy to the load.

An individual cell has a low terminal voltage, typically around 0.5V, and solar panels typically consist of a battery connection of many individual cells in series. A commercial solar panel may have 72 cells connected in series providing an open circuit voltage of around 32V in full sunshine.

The Efficiency of Photovoltaic Cells

The solar spectrum is the total distribution of electromagnetic radiation emanating from the sun and the different regions of this solar spectrum are described by their wavelength or frequency. The visible region extends from about 390 to 780 nm[13] as shown in Figure 13. Around 99 percent of solar radiation is contained in a wavelength band from 300 nm (ultraviolet region) to 3,000 nm (near-infrared region).

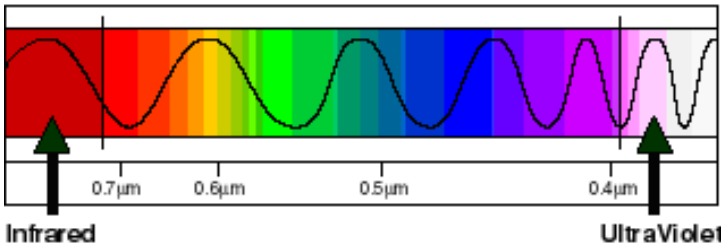

Figure 13: The visible light region of the electromagnetic spectrum

(from http://imagers.gsfc.nasa.gov/ems/visible.html)

The efficiency of a solar cell is the electrical power that it delivers as a percentage of the insolation power that it receives from the incident sunlight. As described in the last section, a fundamental limitation is the bandgap of the material and the energy that is required to excite an electron from the valence to conduction bands. This amount of energy requires to a specific frequency in the light spectrum or colour of light. Photons with less energy than the bandgap pass through the material and those with more energy create just one hole-electron pair with the surplus energy being lost as heat.

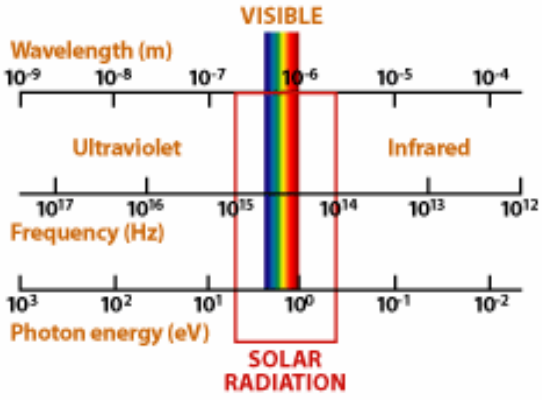

Figure 14: The solar spectrum shown in wavelength, frequency and photon energy

(from http://www1.eere.energy.gov/solar/pv_cell_light.html)

[13] 1nm = 1 x 10^{-9} m (one billionth of a metre)

The solar spectrum can also be represented in terms of frequency (the product of wavelength and frequency is the speed of light) and photon energy (using the Einstein photoelectric equation with Planck's constant) and this is shown in Figure 14. It is now possible to relate the incoming solar energy with the bandgap of the material used in the photovoltaic cell to calculate the theoretical conversion efficiency from light into electrical energy. The maximum theoretical efficiency from a single junction cell is around 30% and this is shown in Figure 15 where some of the common materials used in this application are shown.

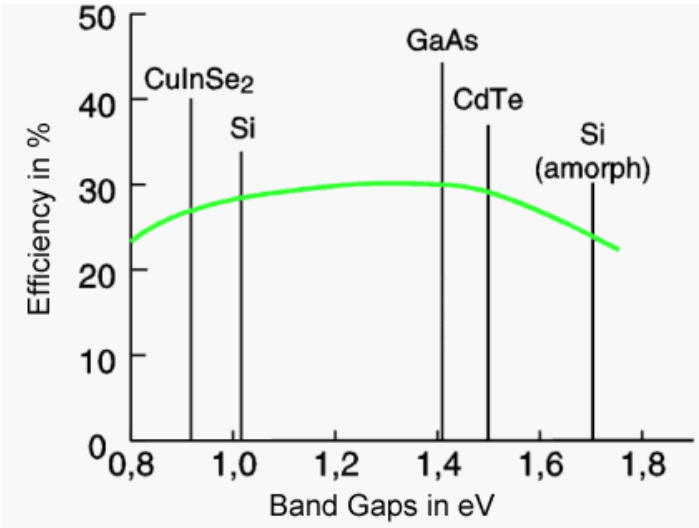

Figure 15: Theoretical conversion efficiencies for PV Cells made from copper indium diselenide ($CuInSe_2$), silicon (Si), gallium arsenide (GaAs), cadmium telluride (CdTe) and amorphous silicon (Si amorph)

(from http://www.solarserver.de/wissen/photovoltaik-e.html)

It is possible to obtain even higher efficiencies with multi-junction cells where a cell is built with several junctions of differing bandgap material to more fully utilize the incoming solar spectrum. The NREL records the efficiency of the best photovoltaic performance obtained in the laboratory and this is shown in Figure 16.

Although the efficiency of a PV cell is not just determined by the bandgap, it is a fundamental limiting factor of the technology. Other factors which impact efficiency and result in practical cells having lower efficiencies than laboratory cells include:

a) Top surface contact obstruction loss – An electrical contact needs to be made to the top surface of the cell which causes light to be absorbed and a loss of active area for the cell.
b) Reflection from the top surface – Any reflection from the top surface reduces the light energy available to the cell.
c) Quantum Efficiency – Not all the incident photons are absorbed by the cell.

d) Collection Efficiency – Not all of the generated hole-electron pairs reach the terminals of the cell, some will recombine within the semiconductor material.
e) Electrical Losses – There are numerous electrical losses within the cell such as series resistance caused by the resistance of the bulk semiconductor material and electrical contacts which dissipate power from the solar generated current.

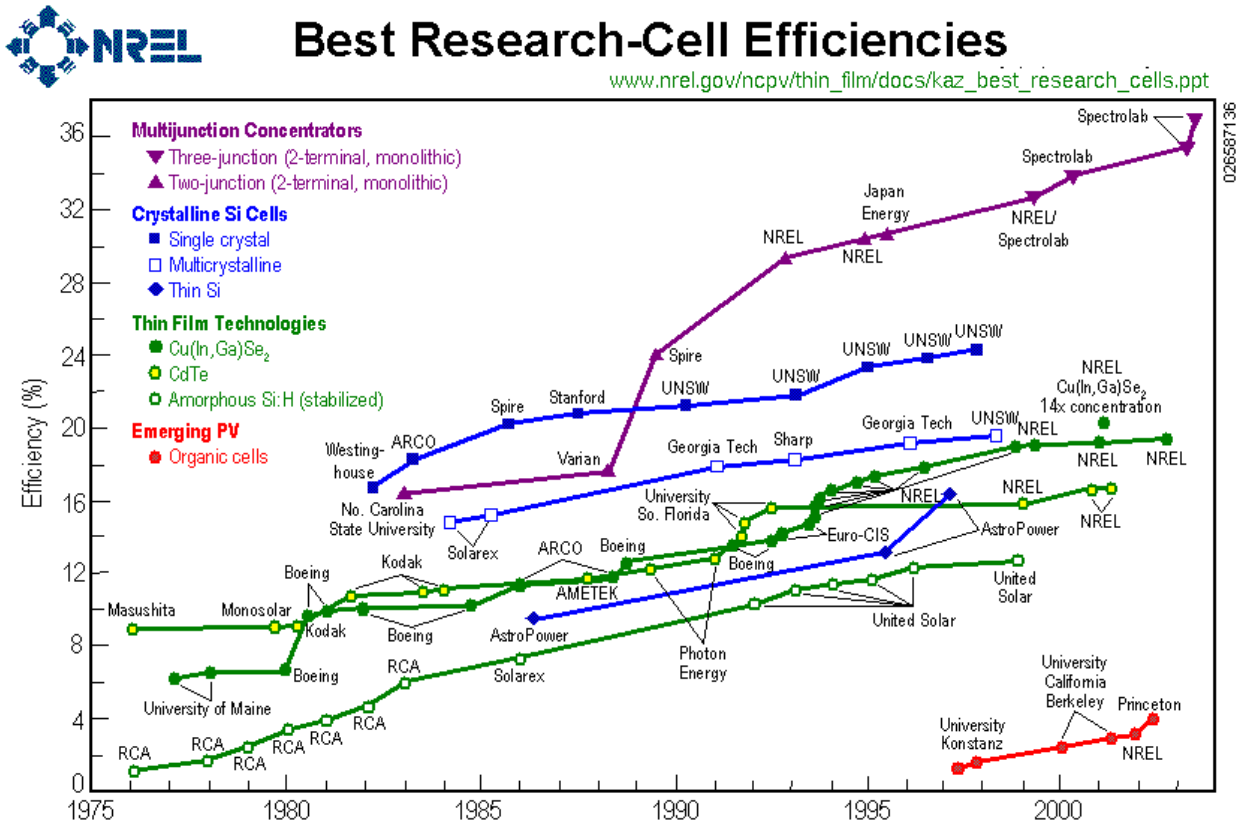

Figure 16: A plot of the best reported laboratory PV cell efficiencies vs year

The principal characteristics of different types of cell in or near to commercial production are summarized in Table 1

Material	Efficiency (%)		Technology
	Commercial products	Best R&D	
Mono- or multi-crystalline	10-18	25	ingot/wafer
Amorphous silicon	5-8	13	thin film
Copper indium diselenide	8	16	thin film
Cadmium telluride	7	16	thin film

Table 1: Solar cell efficiencies achieved by the principal semiconductor technologies

(from Markvart Energy for Europe, 2002)

Commercial Photovoltaic Technologies

Monocrystalline / Multicrystalline Silicon Cell

In producing silicon solar cells, the silicon needs to have electronic grade purity and this has been traditionally manufactured using the Czochralski method. This process uses a crucible containing molten high-purity silicon and a seed crystal, mounted on a rod, which is then dipped into the molten silicon. The seed crystal rod is then pulled upwards and rotated at an appropriate rate to form a large, cylindrical, single crystal, ingot from the melt. This cylindrical ingot can then be cut and polished into wafers. This material has high purity and good performance for electronic devices including solar cells, however it is an expensive process. Consequently the devices built using this method, monocrystalline cells, have good performance with efficiencies in the region of 15% but they are expensive. Monocrystalline cells were the first photovoltaic cells to be mass manufactured for power applications and subsequently there has been extensive development activity to reduce silicon costs.

The multicrystallne technologies normally use some form of casting or ribbon growth method for making the silicon material. Consequently the cells usually have a rectangular section, whereas monocrystalline cells are built from circular wafers and are therefore normally circular in shape; or trimmed to be octagonal for better packing densities when assembled into modules. The relatively large area of the grain size in the multicrystalline silicon (0.1 to 10 cm) result in high efficiency devices somewhat below the performance of monocrystalline cells at around 13%. .

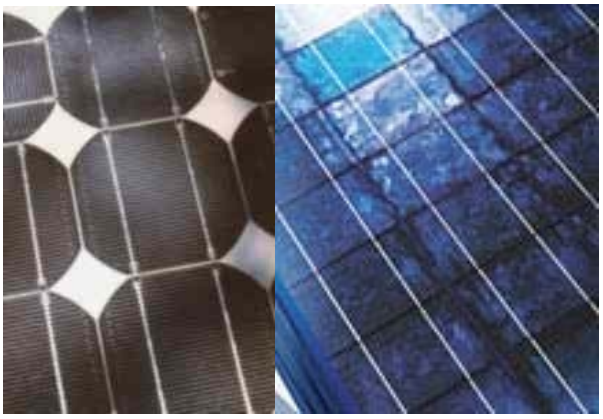

Figure 17: Monocrystalline (left) and multicrystalline (right) PV cells

Note the crystal grains visible on the multicrystalline cells
(mono photo from D. Lenardic, multi photo from Solar-fabrik)

Amorphous Silicon

The high cost of crystalline silicon, which can represent half the cost of a PV module, promoted research into alternative manufacturing methods for solar cells. Amorphous silicon has a different silicon structure and can be deposited as a thin film over a large area onto substrates including glass and metal. Amorphous silicon is more disordered than crystalline silicon with bond angles between atoms which are irregular and with no orderly lattice structure. Consequently the electronic properties of the material are very different with a bandgap of 1.75eV compared to 1.1eV for crystalline silicon. Only about 1 micron of amorphous silicon is required to absorb most sunlight compared to 100 micron of crystalline silicon and this property of strong light absorption is a significant advantage for amorphous silicon as a thin film photovoltaic material (Ref 17).

Thin film production techniques are suited to high volume, and therefore lower cost, manufacturing. The amorphous silicon cells use a slightly different junction structure from the p-n technology explained previously and operate in a similar manner but at a lower efficiency, typically in the range of 7%. As with many thin film technologies, such cells can experience significant degradation in their power output when exposed to sun and this can range from 15% to 35%. Amorphous silicon has a significant share of the photovoltaics market especially where cost is more important than performance.

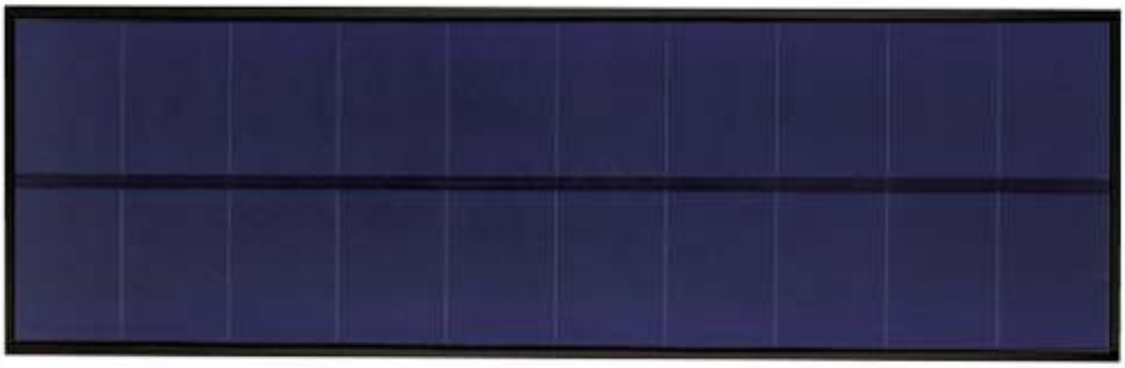

Figure 18: An amorphous silicon PV module

(from United Solar Ovonic)

Other Thin Film Technologies

As is evident from Figure 15 there are other semiconductor materials which offer better photovoltaic performance than silicon which can also be thin film deposited., most notably cadmium telluride (CdTe) and copper indium (gallium) diselenide (often abbreviated to CIS or CIGS). These technologies are complex and have experienced problems with long term stability of the thin film structures. They have taken over twenty years, of development, supported in some cases by major corporations, to get from the stage of promising research to the first manufacturing plants producing early products.

The Dye Sensitised Solar Cell

The dye sensitised solar cell, also referred to as the Graetzel cell, operates on a different principle to the semiconductor PV cells previously discussed. This cell was invented by Professor M. Gratzel and his colleagues at EPFL, Switzerland in the early 1990s and somewhat resembles plant photosynthesis in operation. In this cell, the solar radiation is absorbed by an organic dye, normally containing ruthenium, and this dye is in close contact with a nano-structured, porous film of the wide bandgap semiconductor titanium dioxide (TiO_2). Electrons within the dye complex are excited and are injected into the conduction band of the adjacent n-type TiO_2 film. The front surface of the cell contains a transparent tin oxide coating which connects to the TiO_2 film and this forms one contact to the cell delivering electrons to the external load. The other contact to the cell (counter-electrode) is connected through an iodide/tri-iodide electrolyte to the photo-electrode containing the TiO_2 film and attached dye as shown in Figure 19. When this counter-electrode receives the electron returning from the external circuit, it is able to reduce the tri-iodide to iodide. The iodide diffused through the electrolyte solution to reduce the photo-oxidised dye molecules back to their original state.

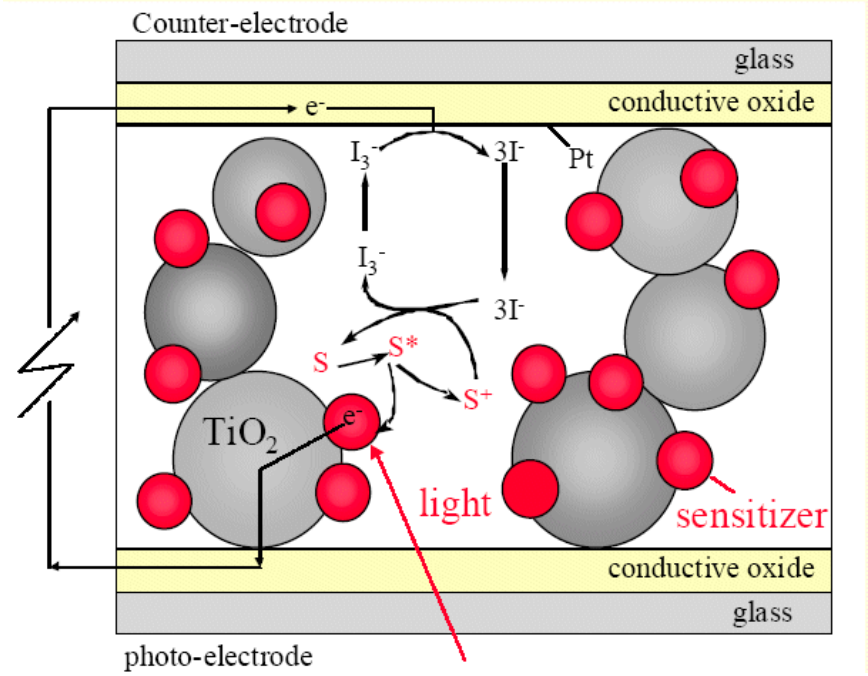

Figure 19: Construction and operation of a nanocrystalline TiO_2 dye sensitised solar cell

(from Flexible Dye-Sensitized Nanocrystalline TiO_2 Solar Cells by Sommeling, Spath, Kroon, Kinderman and van Roosmalen)

Efficiencies of over 10% have been reported with this cell which offers the prospect of relatively low cost, high scale production. However the use of liquids and an organic dye within the cell raise issues with long term performance and reliability.

Technology Choice for Antarctic Applications

Antarctica is not a low-cost environment and reliability, together with ease of operation, is paramount. The crystalline silicon technologies are relatively robust and have a proven record of performance in cold weather environments such as the Arctic and also provide high efficiencies albeit at relatively high cost. The other photovoltaic technologies under development for power generation applications, most notably the thin film technologies, have lower efficiencies although their cost is lower. However there are still technical problems to be overcome with most of these technologies, especially with performance degradation over time, and this is also the case with dye sensitised solar cells. In the Antarctic application, with its difficult operating environment, these technologies are not sufficiently mature to offer a viable solution. Although they are more expensive, the crystalline silicon photovoltaic technologies do offer high efficiency and reliability, their increased cost is probably less of an issue for this application where electrical generation costs are much higher than conventional sites.

Device Characteristics

A PV cell replaces a battery as a source of direct current (d.c.) in an electric circuit and is activated by light whereupon it develops a voltage to drive a current around an external circuit (the load). The voltage developed with no load is called the open circuit voltage, V_{oc}, and the current flow with the cell terminals connected together is known as the short circuit current, I_{sc}. Under illumination, the current versus voltage characteristic of a cell is typically as shown in Figure 20 where V_{oc} and I_{sc} both increase with the light intensity.

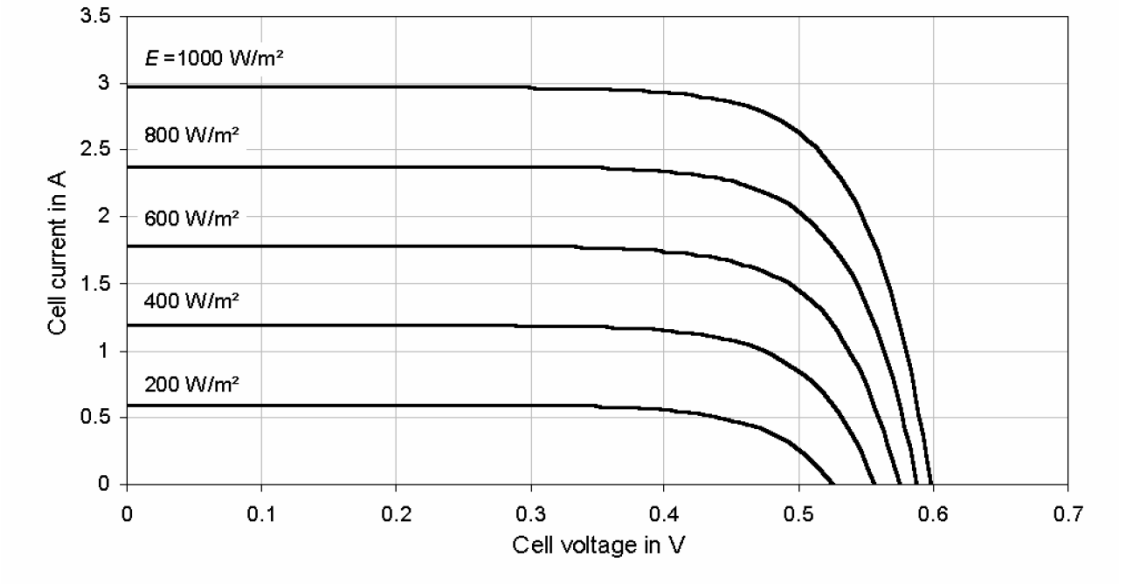

Figure 20: The current vs voltage (I-V) characteristic of a PV Cell under illumination

(from ref 19)

Since power is the product of current and voltage, the power curve can be derived from this characteristic as shown in Figure 21. It can be observed that a maximum power point occurs at the knee of the I-V curve and this represents the optimum operating point of the panel. A Maximum Power Point Tracker (MPPT) is a device which maintains a photovoltaic panel at this operating point, which changes with parameters such as illumination and temperature, to ensure that it will deliver the maximum possible output power.

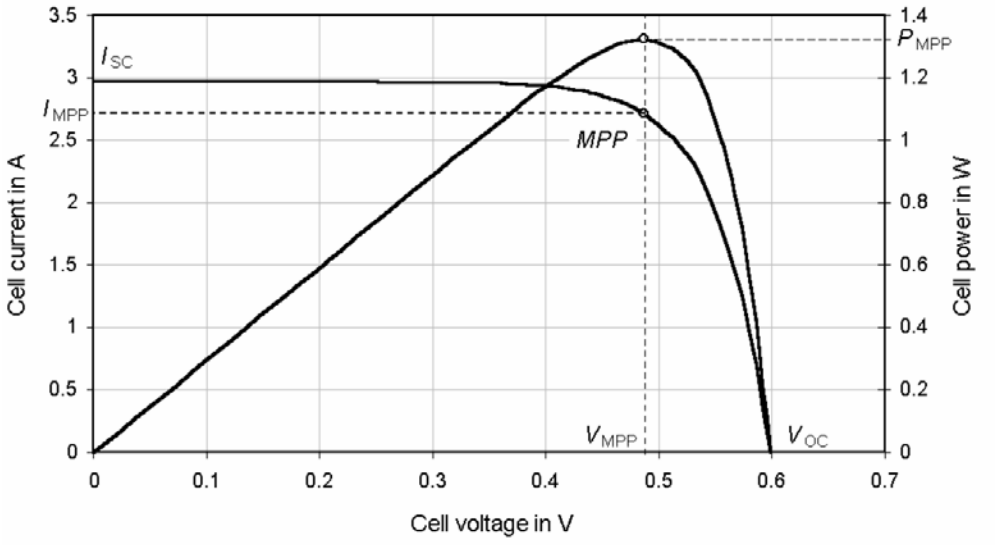

Figure 21: The current vs voltage (I-V) and power vs voltage (P-V) characteristic of a PV Cell under fixed illumination

(from ref 19)

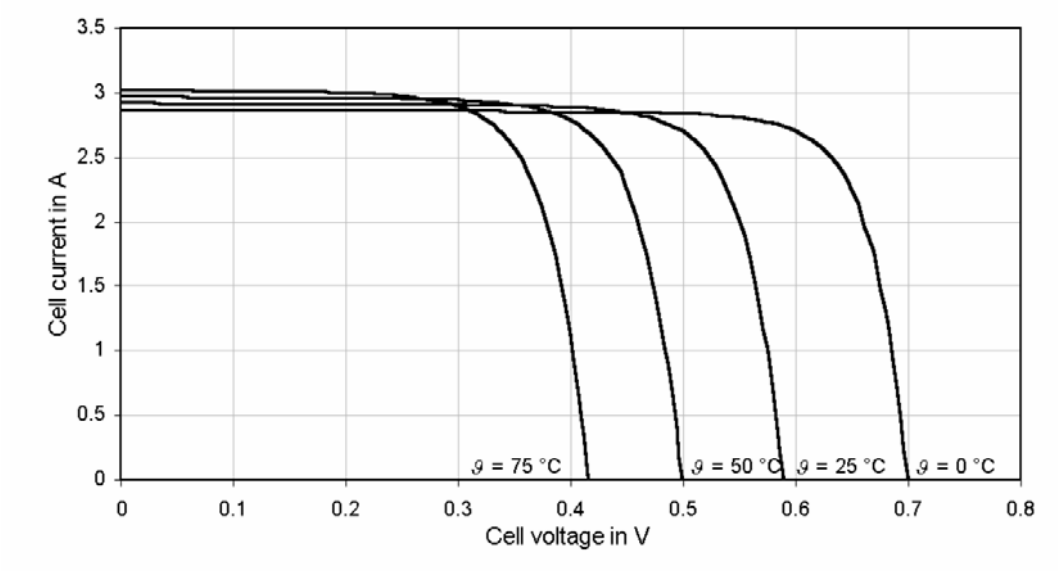

Figure 22: Temperature dependence of a PV cell output characteristic

(from ref 19)

The temperature dependence of the output of a PV cell is shown in Figure 22 and it can be seen that the power increases with reducing temperature. A silicon PV cell has a coefficient of maximum power with temperature of around -0.4%/°C, the power increases by 10% with a 25°C reduction in temperature.

The low operating voltages of PV cells requires large numbers to be connected in series to form modules having reasonable terminal voltages. Consequently if any one of these cells has a reduced output, for example by local shadowing on the module, the overall output can fall dramatically. An analogy would be treading on hosepipe and its effect on the water output from a hose. Modules are constructed to reduce this problem, for example by connecting inverse diodes across each cell within the module, however within the design of a PV system, it is important to reduce shadowing effects.

Comparisons with Existing Projects

In this section, two existing photovoltaic installations, which have both adopted monocrystalline technology, are reviewed. Using insolation data from the NASA SSE web site, the published operational data from these systems has been used to estimate the performance of a similar system at the South Pole.

In the case study of 'Solar is Saving Energy for the Alfred A.Arraj U.S. Courthouse' (ref 20) , a PV installation in Denver, Colorado is described In this application, the PV cells were sandwiched in translucent glass panels and mounted horizontally to form a shaded roofing system. The PV cells were used in three banks with associated inverters, each supplying one phase of power, to a grid connected system without the use of batteries. The system has a planned life of 30 years for the PV panels, 10 years for the inverters and the unit cost was estimated at $10,435/kW which equates to $0.47/kWh. The system has the following parameters:

1) 11.5kW_{dc} rated at standard test conditions
2) 30kWh/day average output
3) monocrystalline modules (Shell/Siemens)
4) Total module area of 110 m^2

A grid connected PV system was installed on the façade of the Nunavut Arctic College in Iqaluit, Nunavut in 1995. The PV cells are mounted vertically on the façade of the college and face 30° west of due south. This system is directly connected to the grid through a single phase inverter with MPPT capability which connects between phases on the building's three phase electrical supply. Nunavut is located at 63.4°N and uses diesel generation for the grid supply and so the application is similar to that which would be required in the Antarctic. This system has produced very useful results on the long term performance of PV arrays at high latitudes, from the published paper (ref 21), the following parameters of the system have been derived:

a) 3.2kWp capacity
b) 2016kWh annual average output (5.5kWh/day)
c) 60 monocrystalline modules (36 Siemens M55, 24 Solec S-53)
d) Total module area of 25.62 m^2
e) Operating temperature range -40°C and 30°C
f) Module efficiency 8-12%

Using these published results, we can compare the two installations:

	Peak Power/Area (Wp/ m^2)	Daily Energy/Area (kWh/ m^2)
Denver	104.5	0.272
Nunavut	124.9	0.215

It can be seen that the peak power of the Nunavut installation is slightly higher than Denver reflecting higher cell efficiency, this may be due to the lower operating temperature together with possible differences in individual cell performance. The daily energy production is higher in Denver due to its higher insolation compared to Nunavut.

The NASA SSE website was used to obtain insolation data for these two locations:

Denver, Colorado

Monthly Averaged Insolation Incident On A Horizontal Surface (kWh/m^2/day)													
Lat 39.75 Lon -104.867	Jan	Feb	Mar	Apr	May	Jun	Jul	Aug	Sep	Oct	Nov	Dec	Annual Average
10-year Average	2.19	2.95	4.11	5.19	6.10	6.57	6.12	5.44	4.84	3.67	2.47	1.95	4.30

Iqaluit, Nunavut

Monthly Averaged Insolation Incident On A Horizontal Surface (kWh/m^2/day)													
Lat 63.4 Lon -68.5	Jan	Feb	Mar	Apr	May	Jun	Jul	Aug	Sep	Oct	Nov	Dec	Annual Average
10-year Average	0.14	0.69	1.77	4.00	5.11	5.33	5.01	3.48	2.16	1.00	0.38	0.07	2.43

With an average insolation of 4.3 kWh/m^2 at Denver compared to 2.43 kWh/m^2 at Nunavut then 4.3/2.43 = 1.76 as much energy would be expected in Denver whereas the previous table shows this factor as 272/215 = 1.26. However the peak power results suggest that the Nunavut PV cells may be more efficient which could be due to many factors such as cell design, placement, shadowing from other structures and ground reflection (albedo) effects. The different orientation of the cells within the two

installations also complicate a simple comparison of performance. Nontheless, these are interesting results since they show relatively close agreement in performance between two similar PV installations.

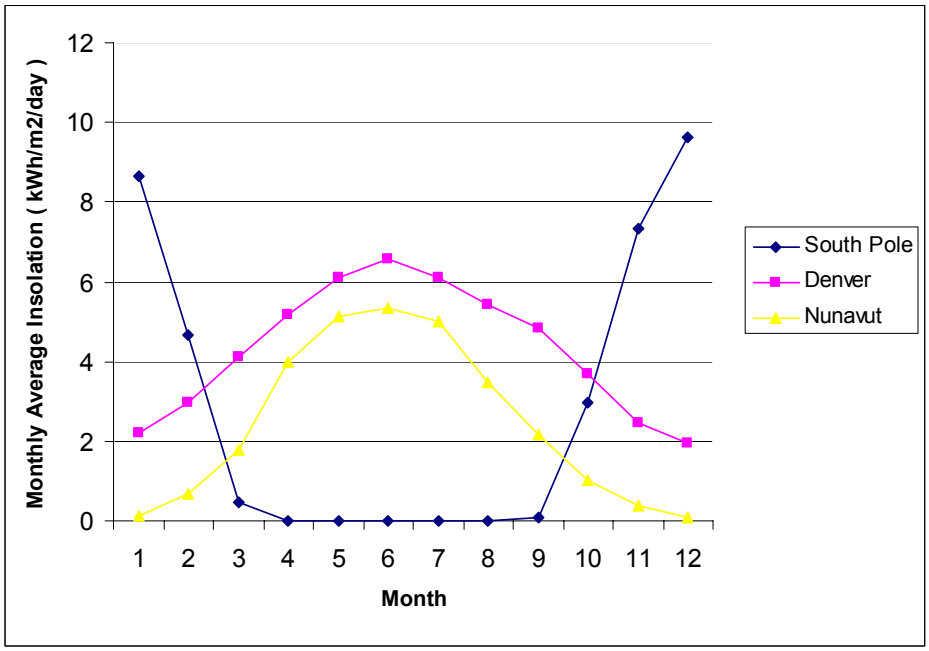

Figure 23: Monthly average insolation vs month for the South Pole, Denver and Nunavut (from NASA SSE website data)

If we take the Nunavut results and extrapolate them to the South Pole, just accounting for the difference in average insolation, then we have:

	Insolation (kWh/ m^2)	Peak Power/Area (Wp/ m^2)	Daily Energy/Area (kWh/ m^2)
Nunavut	2.43	124.9	0.215
South Pole	2.81	144	0.248

Table 2: Insolation, peak power and daily energy per unit area of a PV array at Nunavut and at the South Pole (predicted)

In the Denver case study, the cost of their PV array was given as $120,000 (materials only) which is believed to be a 2003 value, equivalent to $1090/$m^2$ of PV array. The projection of these results to the South Pole would yield $4395 for a daily kWh of energy and if the system was depreciated over 20 years this would equate to $0.60/kWh.

The area of PV array required to provide a continuous kW of power at South Pole Station would be 97m^2 (the Nunavut array provided a continuous 0.23kW of power with 25.62 m^2 of PV area).

Modeling the Solar Resource

Solar Position and Panel Geometry

In designing photovoltaic systems, it is necessary to accurately estimate the amount of sunlight that is available to provide the solar energy input to the system. It is relatively straightforward to predict the location of the sun in the sky at a given time for any point on earth. This information can then be used to calculate the solar insolation on a collector surface, such as a photovoltaic panel. The system can be modeled mathematically and simulated within a computer program such as Matlab[14].

The earth revolves around the sun in an elliptical orbit, making one revolution every 365.25 days. Since the eccentricity of the ellipse is small, the orbit is almost circular and, although the energy output of the sun varies slightly, the energy reaching the earth can be assumed to be constant to a reasonable approximation. The solar constant defines the amount of solar radiation which falls on an area above the atmosphere at a vertical angle and has the value of 1367 W/m^2. In solar energy applications, the characteristics of the earth's orbit are considered to be unchanging.

The earth's spin axis is currently tilted at 23.45° with respect to the elliptical plane of orbit around the sun which causes the earth's seasons. On March 21 and September 21, or 22 of the month for a leap year, a line from the centre of the sun to the centre of the earth passes through the equator and everywhere on earth has 12 hours of daytime and night, this is the equinox. At the poles, the equinox marks the division between the periods when the sun does not set (polar day) and when it does not rise (polar night).

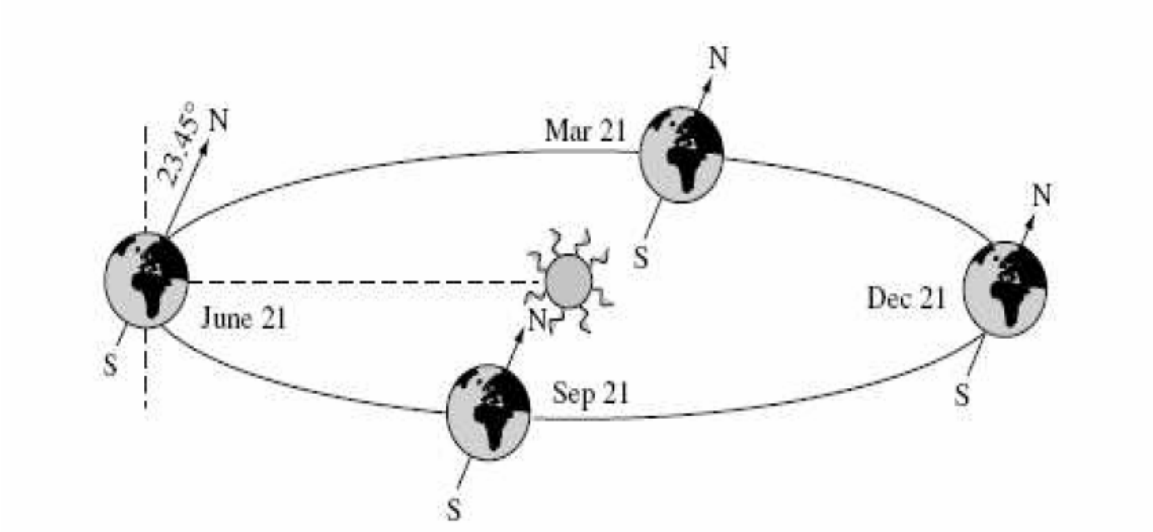

Figure 24: The orbit of the Earth around the Sun

(from ref 22)

[14] Matlab is a registered trademark and product of The MathWorks, Inc.

At a fixed point on earth, the sun's movement across the sky can be represented in terms of several angles:

(1) The solar zenith angle (α) is the angle between the incident solar beam and a line at 90°[15] to the earth's surface (called the zenith).
(2) The solar altitude angle (β) is the complement of the zenith angle being defined as the angle between the incident solar beam and earth's surface ($\beta = 90° - \alpha$).
(3) The solar azimuth angle (Φ_s) is the angle between a reference longitude on the earth's surface and the plane defined by the incident solar beam and zenith. The solar azimuth is referenced to south in the northern hemisphere and north in the southern hemisphere with angles towards east being defined as positive and angles towards west as negative.

The location of the sun at any time of day can be defined in terms of the altitude angle and azimuth angle. These angles depend on the latitude, day number (position of the day within the year) and the time of day.

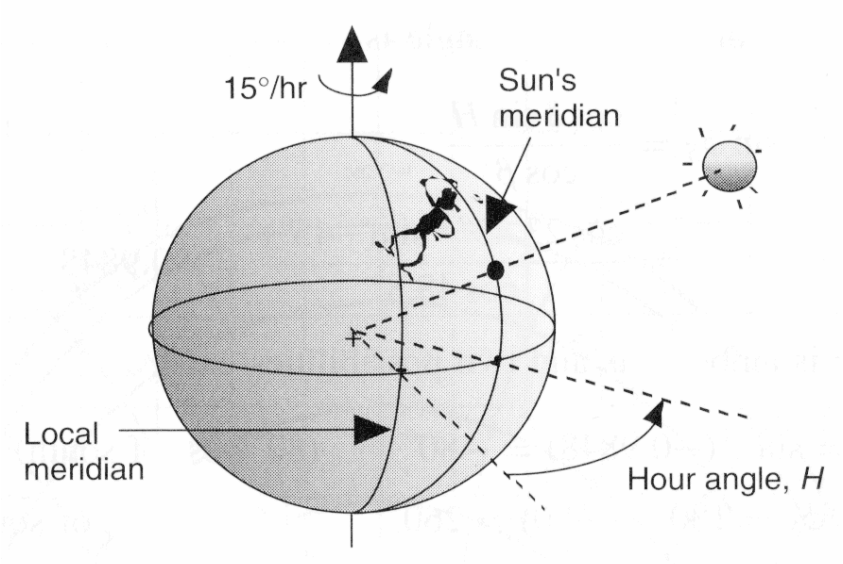

Figure 25: The solar hour angle is the angle the earth must turn before the sun is over the local meridian

(from ref 23)

The solar hour angle is the angle between the local longitude and the sun's meridian as shown in Figure 25. Since the earth rotates 360° about its own axis each day, the solar hour angle changes at a rate of 15°/hour and can be described as:

Hour angle H = 15° x (hours before solar noon)

[15] A line at 90° to a surface is described as being perpendicular or normal to that surface

As an example at 11am solar time, the hour angle would be +15° as the earth needs to rotate another 15° before it is solar noon.

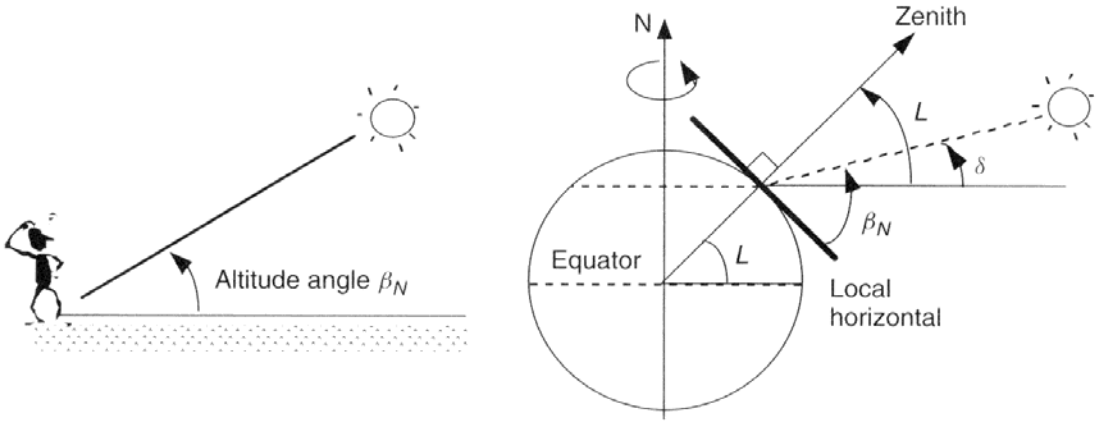

Figure 26: The altitude angle of the sun at solar noon

(from ref 23)

The altitude angle of the sun at solar noon can be calculated from basic geometry using Figure 26 and shown to be:

$B_N = 90° - L + \delta$

Where L is the latitude of the location and δ is the solar declination which is the angle formed between the plane of the equator and a line drawn from the sun to the centre of the earth.

Since the earth's axis is tilted with respect to the sun and the earth is also orbiting the sun, the solar declination changes over the year between the extremes of ±23.45° (the earth's tilt angle). A sinusoidal relationship which assumes a 365 day year with the spring equinox placed at day n = 81 provides a good approximation and the solar declination angle can be expressed as:

$\delta = 23.45 \sin [360(n - 81)/365]$

Knowing the solar hour angle H, latitude L and solar declination δ, it is possible to derive equations for the altitude (β) and azimuth (Φ_s) angles of the sun (see ref 25):

$\sin \beta = \cos L . \cos \delta . \cos H + \sin L . \sin \delta$

$\sin \Phi_s = (\cos \delta . \sin H) / \cos \beta$

A solar panel is a flat, plane surface with an azimuth angle defined by Φ_c and an elevation or tilt angle defined by Σ as shown in Figure 27.

The incident angle of the beam to this panel, θ, can be calculated in terms of the solar panel angles, Φ_c and Σ, together with the solar angles, β and Φ_s, using the equation:

$$\cos\theta = \cos\beta \cdot \cos(\Phi_s - \Phi_c) \cdot \sin\Sigma + \sin\beta \cdot \cos\Sigma$$

This allows us to calculate the component of the solar flux which is normal to the panel and which can be converted into electricity (more details of its derivation are in ref 24).

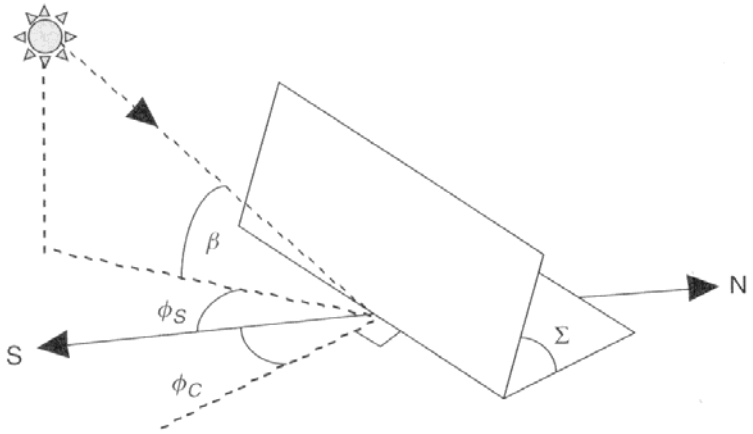

Figure 27: Panel azimuth angle and elevation (tilt) angles along with the solar azimuth and altitude angles

(from ref 23)

Incident Solar Flux

The sun acts, to a good approximation, as a perfect black body emitter of radiation and the resulting average energy flux incident on a unit area which is perpendicular to the beam outside the earth's atmosphere is 1367 W/m^2 (the solar constant).

The amount of radiation that reaches the ground is extremely variable, in addition to the location of the sun described in the previous section, variations are caused by climatic conditions, such as cloud cover, and the general composition of the atmosphere. Typically about 300 W/m^2 is lost to reflection and atmospheric absorption such that on a sunny day at noon around 1000 W/m^2 of sunlight is available at the earth's surface for conversion into electricity by a PV system as shown in Figure 28.

The concept of air mass is used to represent the ratio of the distance the solar beam travels in the atmosphere at a given sun angle compared to when the sun is directly overhead at noon as shown in Figure 29. The radiation from the sun at zenith corresponds to air mass 1 (abbreviated to AM1) and at other times, the air mass, m, is given by:

$$m = 1/\cos\alpha$$

where α is the zenith angle.

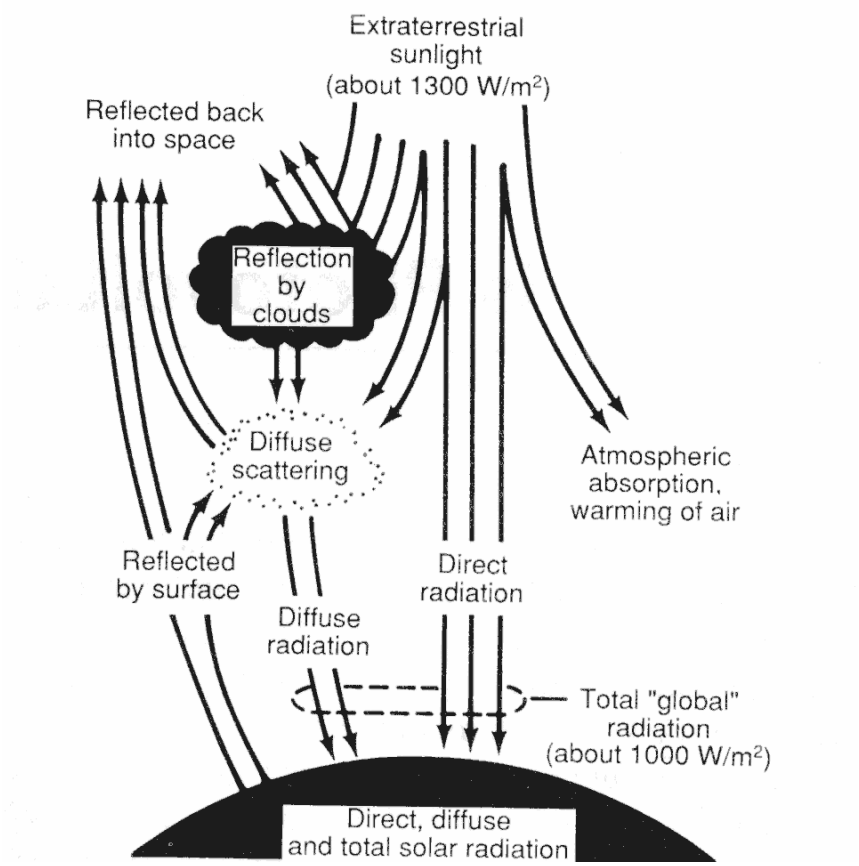

Figure 28: The path of extraterrestrial sunlight through the atmosphere

(from ref 18)

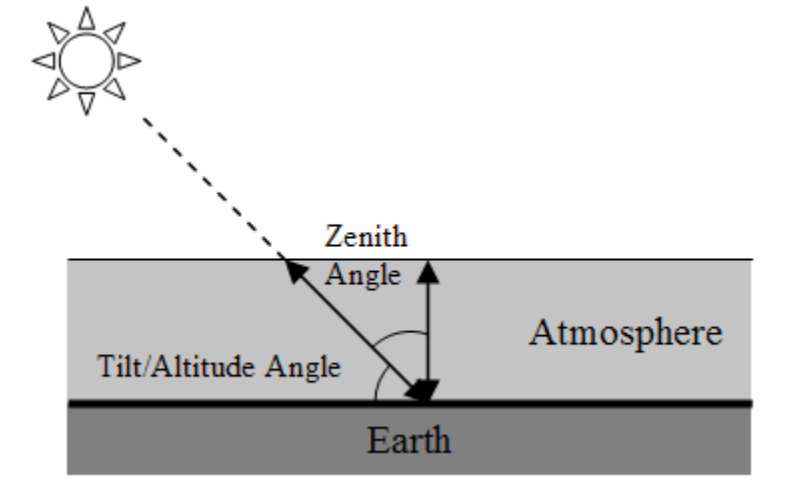

Figure 29: Flat earth air mass geometry

The attenuation of incoming solar radiation under clear sky conditions is a function of the distance that it has to travel through the atmosphere and it can be calculated using an exponential decay function. If the beam portion of the incoming radiation is I_B then:

$I_B = A. e^{-km}$

where A is the 'apparent' extraterrestial flux, k is a dimensionless factor called the optical depth and m is the air mass ratio.

The American Society of Heating, Refrigeration and Air Conditioning Engineers (ASHRAE) provide tables for the 'apparent' extraterrestial flux and optical depth. Using these tables, an average value of A and k were estimated. In the South Pole situation with clear skies and low humidity, the 'apparent' extraterrestial flux would be close to the solar constant.

Albedo Radiation

Another source of light energy for PV arrays is the reflected light from the ground and other objects near the array. The albedo is the ratio of the sunlight reflected by a surface to the incident sunlight onto that surface and typical values are shown in Table 3. This table provides a range of albedo for each type of surface since the exact value depends on parameters such as the surface texture and angle of incidence.

Surface	Typical Albedo
Fresh Snow	0.7 – 0.9
Aged Snow	0.6 - 0.8
Ice	0.4 – 0.5
Melting Snow	0.3 – 0.4
Soil	0.1 – 0.4

Table 3: Typical albedo of some common materials

(from ref 26)

In the calculation of PV performance at South Pole Station, the effect of albedo radiation has not been included, it will obviously increase the output of PV systems with panel tilts which offer a path for albedo radiation.

Photovoltaic Panel Performance

The output of the photovoltaic array was simply calculated from the incoming solar radiation using a conversion efficiency of 13% which represents the performance of a modern crystalline solar cell (ref 28). A power coefficient of temperature of -0.43%/°C was used to correct for the operating ambient temperature.

The Matlab Model

The Matlab code estimates PV panel power by:

(1) Calculating sun position across a given time period for a given latitude, longitude and altitude using an implementation of an algorithm developed by Reda and Andreas of the NREL (ref 27).
(2) Calculating the incoming solar radiation for a particular panel tilt and azimuth angle using an exponential decay function to model atmospheric attenuation.
(3) Calculating the electrical output for this incoming solar radiation assuming an ambient temperature of -21°C.

In running these simulations, the time span selected was 23 September 2006 to 21 March 2007 which covers the current Antarctic austral summer. A plot of the sun altitude angle versus day is shown in Figure 30.

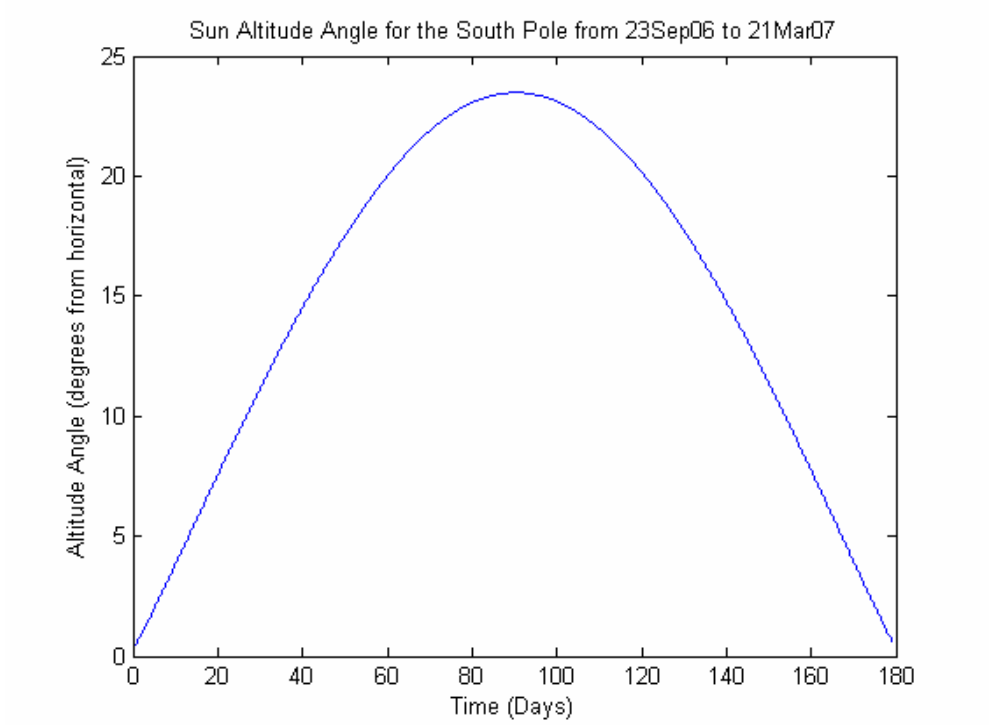

Figure 30: Matlab simulated sun altitude angle for the South Pole from 23 Sep 2006 to 21 Mar 2007

On the NASA SSE website, it is also possible to plot the daily averaged insolation for a time period over a selected range and this is shown for the year of 1991 in Figure 31. The next step was to run a simulation to calculate incoming solar radiation and the daily averaged insolation, this is shown in Figure 32. As can be seen, the simulated results are slightly lower than the NASA results which may result in the simulation results being somewhat conservative for PV output powers. The corresponding plot of solar power

received at the panel over 20 minute intervals for this period is shown in Figure 33 and can be seen to peak at over 800W/m^2. This is for the optimum panel angle of 60° which was calculated from a later simulation.

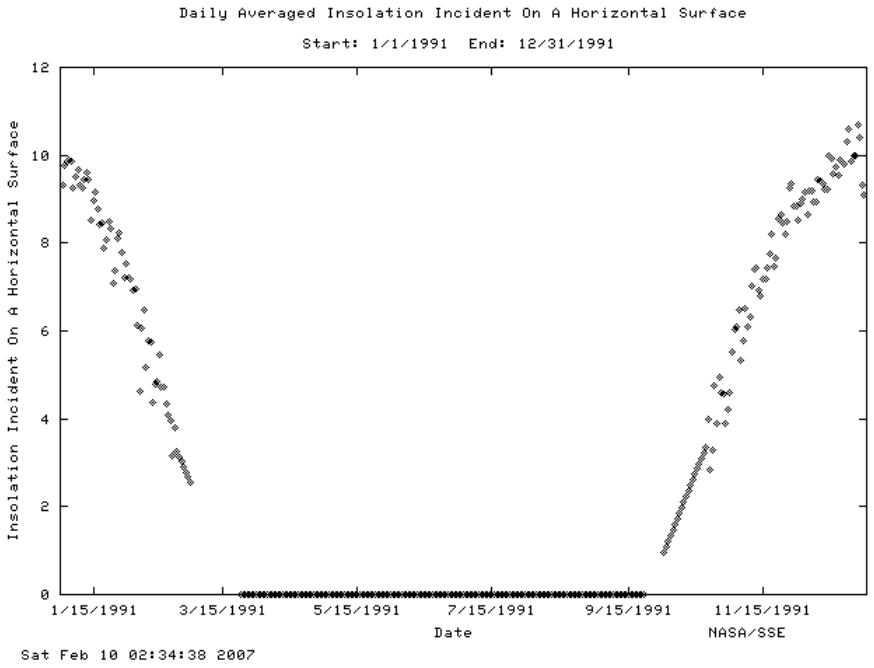

Figure 31: Daily average insolation (kWh/m^2) on a horizontal surface for 1991

(from the NASA SSE website)

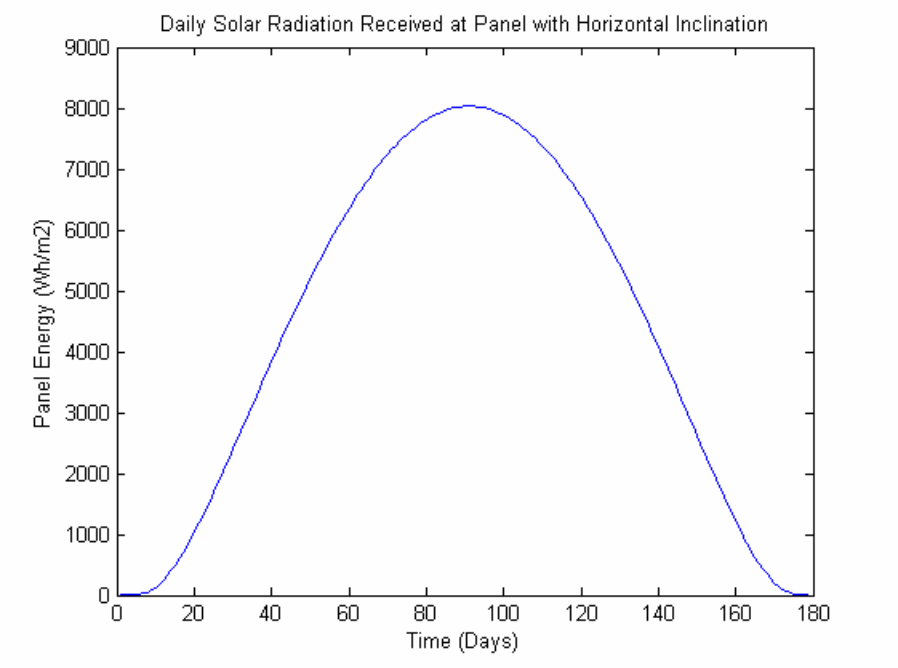

Figure 32: Daily average insolation (Wh/m^2) on a horizontal surface from Matlab simulation

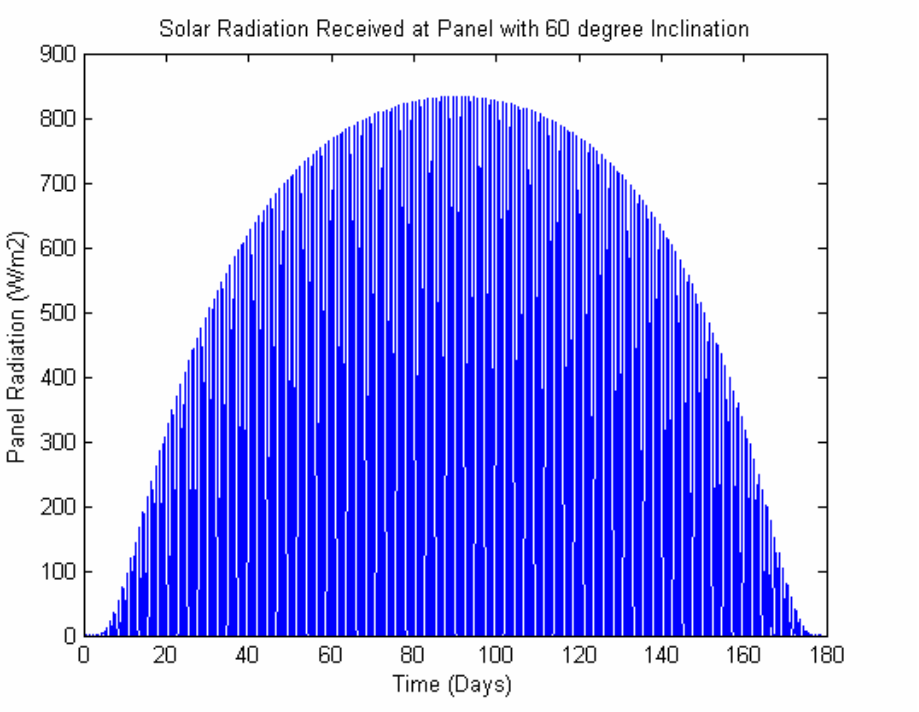

Figure 33: Solar power received at a panel with optimal 60° inclination

The final step is to run the simulation to calculate the panel power for a given panel azimuth and inclination. In the case of the South Pole, the panel output for a horizontal panel is shown in Figure 34:

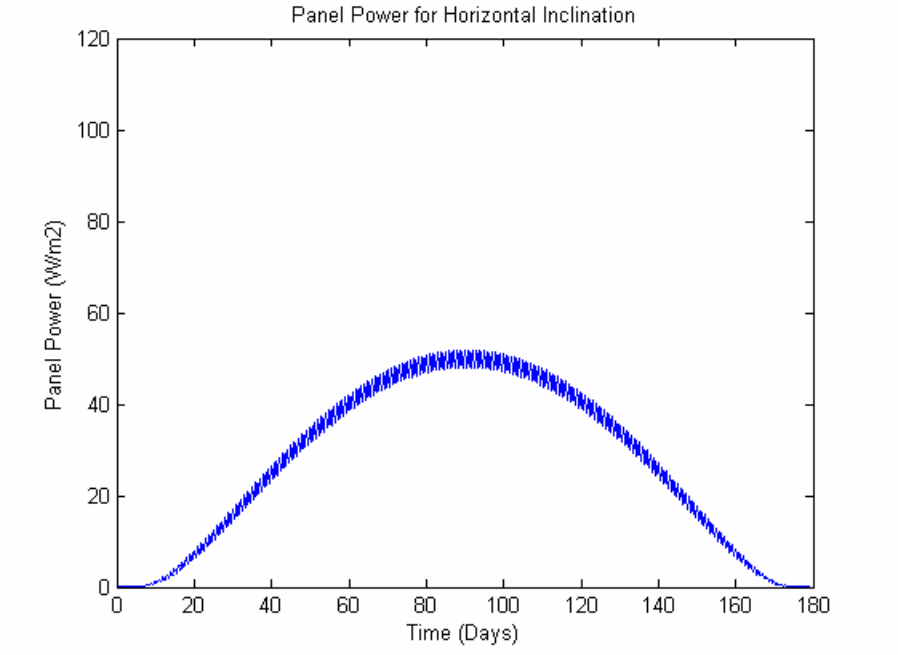

Figure 34: Panel power for a horizontal panel

The panel power for calculated optimal inclination is shown in Figure 35 and a plot of panel power vs panel inclination is shown in Figure 36; the peak at 60° corresponds to the optimum interception of insolation.

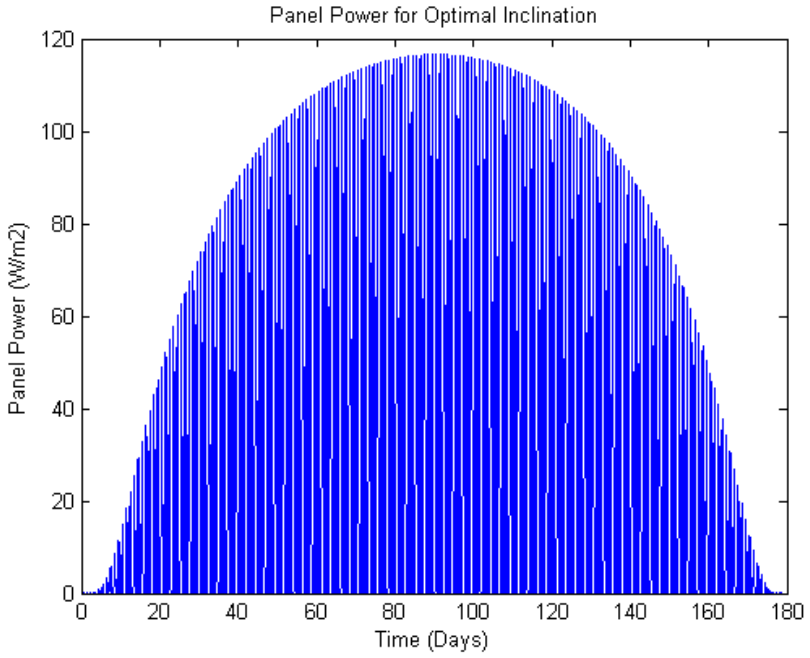

Figure 35: Panel power for the optimal panel inclination of 60°

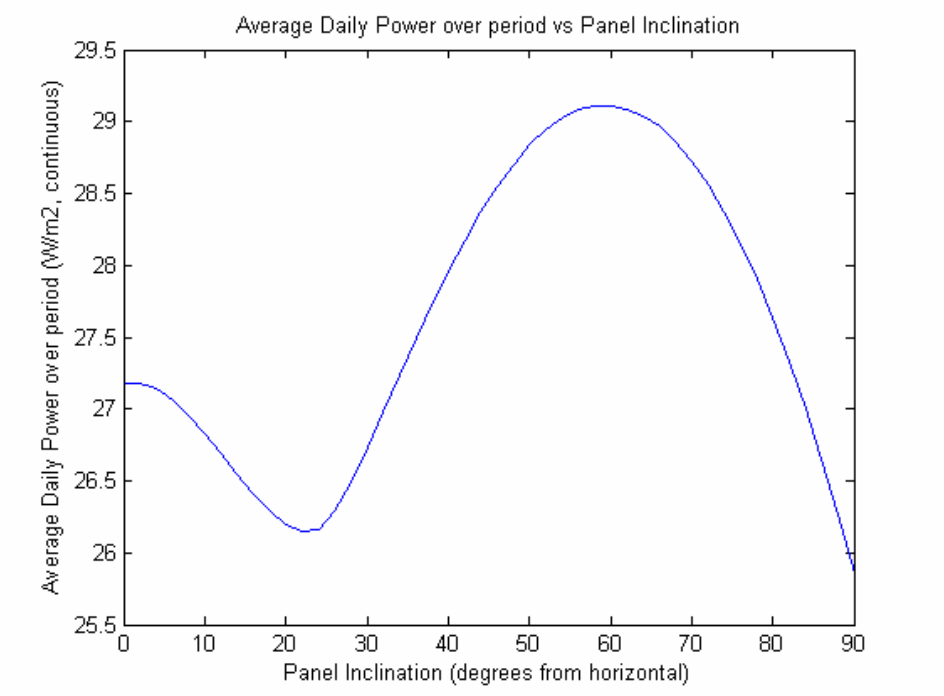

Figure 36: Average daily power vs panel inclination angle (averaged over the 180 day period)

An Initial Implementation at South Pole Station

The elevated building at South Pole Station provides a convenient structure onto which PV panels could be mounted. This would probably provide the easiest implementation of a PV system at South Pole Station, taking advantage of an existing structure and would also enable convenient connection into the station's power grid. The three most practical face areas, shown in are given as the north face of 1770 sq ft (164.4m^2), west face of 565 sq ft (52.4m^2) and east face of 562 sq ft (52.2m^2) providing a total area of 269 m^2 as shown in Figure 37.

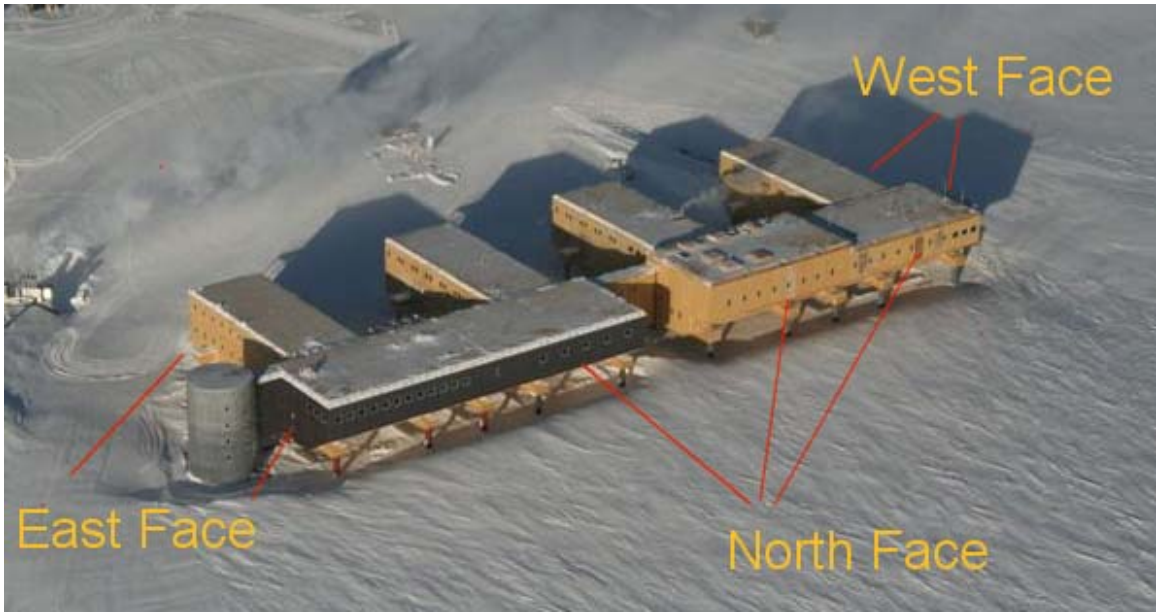

Figure 37: The elevated building at South Pole Station

Assuming a PV panel coverage of 80% of the available area and vertical mounting of the panels, the following energy yields would be possible based on the Nunavut case study results and the Matlab simulation:

	Daily Averaged Energy (over full year)			
	Panel (kWh/m^2)	North Face (kWh)	West Face (kWh)	East Face (kWh)
Nunavut	0.215	28.27	9.01	8.97
Matlab	0.279	36.69	11.69	11.65

Table 4: Predicted PV panel energy outputs for installations on the vertical walls of the SPS elevated station

Note: From Figure 36, the daily averaged power over a 180 day period for a vertically mounted panel is 23.6W which translates to 566Wh/day and converting this to a 365 day year provides 279Wh/day.

These results show a good correlation with the Nunavut case study but predict a higher energy output which would be expected for the South Pole since it is a better solar site. The NASA SSE data gives the daily average insolation at Nunavut as 2.43 kWh/m^2/day and at the South Pole as 2.81 kWh/m^2/day. Hence a PV system at the South Pole should generate 15% more electricity compared to Nunavut with the same panel efficiency and temperature.

The panel efficiency at Nunavut is around 10% (figure 6, ref 21) compared to 13% in the South Pole simulation which would result in 30% more energy being generated between the case study and simulation. According to the NASA SSE website, the summer operating temperatures at South Pole Station are around 22°C cooler than Nunavut which would result in an increased PV power of about 9.4%. Accounting for these differences would increase the insolation result of 15% to 63% for the final PV energy output, the panel energy values from Table 4 yields 29%. The simulation is midway between the case study and an estimation derived from the environmental differences between the two sites.

Using the Matlab simulation, the panel power output for a vertically mounted panel is shown in Figure 38:

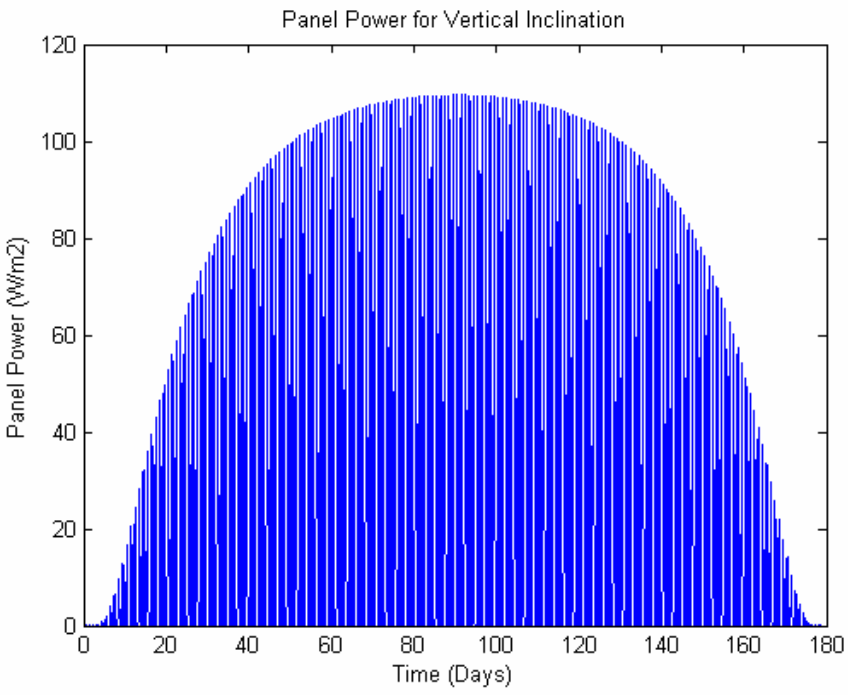

Figure 38: Panel power for a vertical panel

The vertically mounted panel sees a higher peak radiation but this fluctuates during the day as the sun moves around the sky whereas the horizontally mounted panel, shown in Figure 34, has continual sight of the sun but with lower, more constant radiation.

	Daily Averaged Values (over full year)			
	Panel Energy (kWh/m^2)	Panel Peak Power (kW/m^2)	PV System Daily Energy (kWh)	PV System Peak Power (kW)
Matlab	0.279	0.109	60	23

Table 5: Matlab simulation results for a vertical wall-mounted PV system at South Pole Station

(showing the panel energy and peak power per unit area of panel; and the energy produced and peak power output of the full system - energy values are averaged over the full year)

The PV installation over this area would provide a peak output power of 23.4kW with a daily energy resource of 60kWh or a continuous 2.5kW of power.

In Energy Costs at South Pole Station, the fuel required to generate a continuous kW of electricity was estimated at 608 gallons, consequently this PV installation should save around 1520 gallons of fuel annually.

At this reduction in load from the main generators, it is probably not necessary to correct for the reduced waste heat coming from the generators. Also PV output will coincide with solar heating and therefore reduced heating demand at the station.

Cost Estimation

The cost of a Power Max Ultra165-PC array is $815[16]

A PV array of $269m^2$ would require 204 of these modules at a total cost of $166,260

An estimate of $100/module for wiring and mounting hardware would total $20,400

The cost of a Ballard Ecostar 30kW power converter is $27,500[17]

The cost of additional hardware for connection into the SPS grid is estimated at $5000

Total materials cost for the project is $219,160

The cost of installation is likely to take the overall cost to around $250,000

[16] http://www.solarhome.org
[17] http://solarhome.org

Assuming a 20 year lifetime for this equipment then it will generate a total of 60*365*20 = 438,000 KWh of electricity.

This translates to a cost of $0.57/kWh over this period.

This result is very similar to the cost of $0.60/kWh given for the Denver case study in Comparisons with Existing Projects. The cost of transportation of materials to the South Pole has not been included, however this is unlikely to significantly alter this result.

Extending the PV System

The previous analysis shows that PV systems are economically viable at South Pole Station but that large areas are required to generate significant amounts of energy. The aerial photograph of the elevated station in Figure 37 shows a significant area of roof space which could be utilized for PV resource. The plot of daily average power versus inclination angle in Figure 36 also shows that slightly more power can be achieved with a horizontal panel at around 27.1W/m^2 compared to 23.6W/m^2 for a vertical panel.

At the elevated station, shown in Figure 39, each "finger" is about 100'x 38', and the two linear sections A2/A3 and B2/B3 are each about 185'x48'[18]. This correspond to a finger area of 352.9m^2 and a linear area of 824.8 m^2.

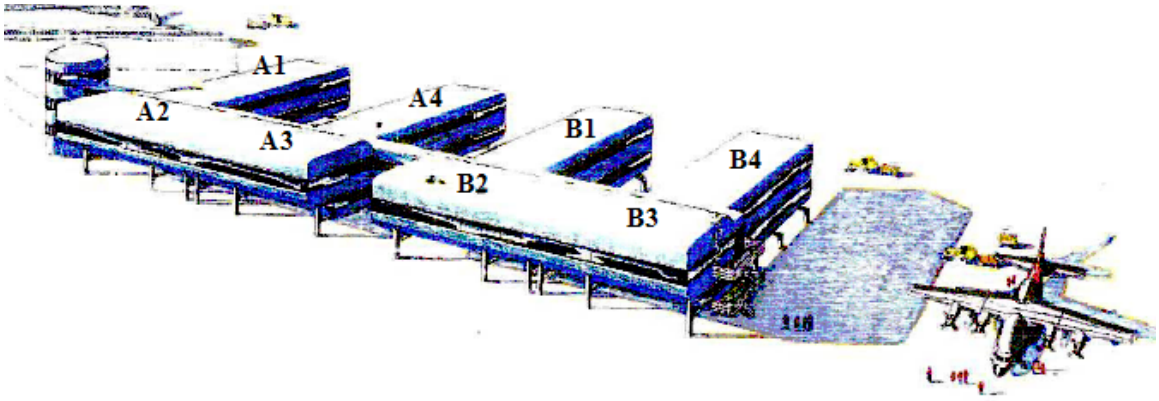

Figure 39: A drawing of the elevated building at South Pole Station with building numbers shown

(a modified drawing from an original by T. Vaughan)

The annual daily power output of 27.1W/m^2 over the summer period corresponds to an annual daily average energy of 0.320 kWh/m^2. Assuming 80% coverage of the roof space with PV panels then the following energy production is possible:

[18] From http://www.southpolestation.com/newpole/newpole.html

Finger Roof = 0.8 * 0.32 * 352.9 = 90.34 kWh/day (a continuous 3.76 kW)

Linear Roof = 0.8 * 0.32 * 824.8 = 211.14 kWh/day (a continuous 8.79 kW)

From Figure 34, the peak output power from a horizontal panel is 52W/m^2 so the peak power outputs would be:

Finger Roof = 0.8 * 0.052 * 352.9 = 14.68 kW

Linear Roof = 0.8 * 0.052 * 824.8 = 34.31 kW

The system could conveniently be divided into four section with each section comprising of a finger PV array and half of the linear PV array (for example the PV modules covering A1 and A2) which would provide a maximum peak power of 32kW.

If the total PV potential of the roof space was realized then a total energy production of 783.64kWh/day or 286,028kW/year would be possible with a peak power of 127.34kW. The installation would provide a continuous power of 32.62kW equating to a fuel saving of around 19,832 gallons (assuming that no fuel was required to make up waste heat lost from the generators).

In Figure 6, it was calculated that providing a continuous 1kW of electrical power at South Pole Station equated to 0.171 LC-130 flights per year. Consequently this system would save over five LC-130 flights per year.

Scaling the previous cost estimate using PV peak power outputs, the cost of this full system would be in the region of $2.8 million. However an advantage of PV technology is its scalability, the installation could be gradually introduced with perhaps the single section covering a roof area such as A1 and A2 being tested first to confirm the predicted performance of the system.

	Daily Averaged Values (over full year)			
	Panel Energy (kWh/m^2)	Panel Peak Power (kW/m^2)	PV System Daily Energy (kWh)	PV System Peak Power (kW)
Matlab	0.320	0.052	783	127

Table 6: Matlab simulation results for a horizontal roof-mounted PV system at South Pole Station

(showing the panel energy and peak power per unit area of panel; and the energy produced and peak power output of the full system - energy values are averaged over the full year)

Note: The design of the elevated station includes various aerodynamic features to reduce snow accumulation around the building. Consequently, the proposed PV implementations

should not change the existing shape of the building significantly. However if panel tilts could be incorporated without adverse effect on the intended aerodynamic properties of the building then some further improvement could be achieved.

Other Considerations

Albedo

The effect of albedo radiation has not been considered for these simulations, although it could be included. In the case of the vertically mounted panel application, it could significantly increase the output from the PV array. The area in front of the elevated station is relatively unobstructed and could provide a useful source of albedo radiation.

Tracking systems

Tracking systems orientate the PV array towards the sun to achieve optimum insolation for the panel, there are essentially three different types of system which fall into the categories of 1-D and 2-D trackers. In the case of 1-D trackers, the array either tracks the azimuth or elevation angles (keeping the other angle fixed). Whereas 2-D trackers adjust both the tilt and azimuth angles such that the angle of incidence of the panel to the solar beam is kept at 0°. However, the complexity of these systems and their reliability make them unattractive for Antarctic applications, better value is likely to be obtained in growing the size of a fixed array rather than investing in a tracking system.

Ageing Characteristics of Modules

There is considerable literature on the ageing of single and multicrystalline PV cells and these cells have clear advantages over other technologies in this respect. However some of the environmental extremes of the South Pole, such as high levels of UV radiation and extreme cold, could have an impact on the long term performance of a PV system which would need to be assessed. This is probably more important for some of the plastic compounds that are typically used in the construction of PV modules rather than for the cells themselves, however other published work in this area (ref 29) is encouraging.

Delivering PV Generated Power

Since the PV array would be grid attached to the main supply at South Pole Station, the MPPT/inverter system which delivers the d.c. power from the PV array to the a.c. supply of the power grid will need to track the supply frequency of the diesel generation system.

The frequency stability of the system would need to be checked to ensure that the MPPT/inverter can track the required range. It will also need to reliably disconnect the PV array from the grid when there is an interruption on the main supply. The integration of the PV system into the power system of South Pole Station would need to be carefully considered for efficiency and security of supply.

PV Array Maintenance

During its operational life, some maintenance may be required on the PV arrays, for example removing ice accumulation which may needed to be manually removed. Normally ice and snow will quickly melt from a PV array due to the dark colour of most PV technologies as shown in Figure 40, however there may still be issues in the extreme environment of South Pole Station. Consequently some form of maintenance procedure would be required, which could possibly be automated, to ensure that the array was operating at full efficiency.

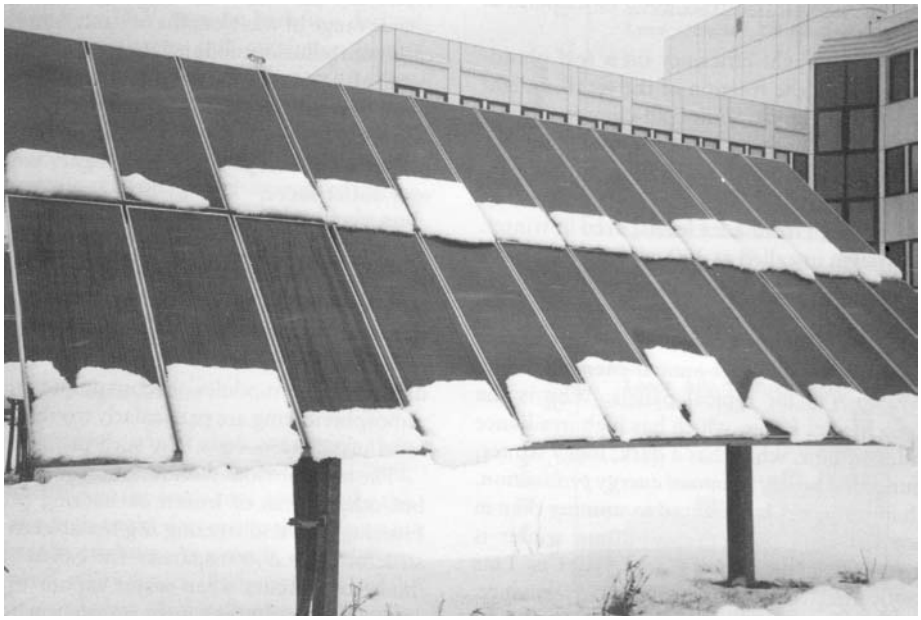

Figure 40: Snow melting off a PV array at Linz, Austria

(from ref 26)

Conclusions

The use of photovoltaic energy generation appears to be economically viable at South Pole Station based off projections from PV installations elsewhere in the world and computer simulation of PV performance at this location. The current electrical generation costs are estimated at $1.39/kWh based on just the fuel costs; the capital depreciation and maintenance costs of the Caterpillar generation system would clearly increase this figure. Conservative estimates for a PV system assuming commercial single/multicrystalline silicon modules would place the cost of PV generation at around $0.60/kWh based on a twenty year depreciation of the system. There are manufacturers who are now guaranteeing their module performance for twenty years or more in conventional terrestrial applications.

Although there are now several commercially available photovoltaic technologies, and more under development, initial research would suggest that mono or multicrystalline technology still offers the best solution for a South Pole implementation. This technology provides relatively high efficiency and being a monolithic technology is inherently more robust for the extreme environment of the Antarctic. This technology provides increased power efficiency with reducing temperature which is a worthwhile advantage and has a proven performance in applications within the Arctic environment. The higher levels of ultra-violet radiation and other environmental extremes at South Pole Station would need to be investigated but since this technology has also been used in satellite applications, it is likely to be capable of long-term Antarctic operation.

A particular advantage of PV technology is that it can be implemented in a scaled manner and a system could be introduced on a small scale and then increased as its operational benefits are proven. The use of PV panels on the elevated buildings at South Pole Station appears particularly attractive, taking advantage of an existing structure and producing electricity close to the area of demand thereby reducing transmission losses. Although generation efficiencies can be improved by more elaborate systems, such as tracking schemes, the extra cost and complication is likely not to be justified in the South Pole application where reliability and ease of operation are more important. It may also be the case that the extra marginal cost of such systems would be better spent on increasing the size of a fixed array in this application.

Photovoltaic technology can be seen to provide a useful and cost competitive supplement to the existing diesel generation plant. It can also provide an additional and independent source of power during the summer months, improving the reliability of supply to the station. The PV generated electricity can be supplied directly into the power grid of the station. This direct grid connection without any form of energy storage, for example batteries, is attractive and will be reflected in savings from generator fuel consumption. There are may also be other opportunities for optimizing the value of this generated energy using load scheduling or in the charging of existing battery installations

Another advantage of a supplementary power source using alternative energy sources is that it frees up LC-130 transport flights to South Pole Station. The availability of LC-130

aircraft is already critically constrained in the Antarctic and these aircraft could be better deployed in other tasks rather than delivering fuel. The South Pole traverse offers some solution to the LC-130 bottleneck but also comes with high economic and environmental costs. In comparison, implementing photovoltaic systems at South Pole Station offer a low risk, cost competitive partial solution to this problem. There are also likely to be other schemes including energy conservation and other alternative energy systems which could offer further relief.

A commercially viable installation at South Pole Station has been outlined which has the potential to pay for itself within eight years but which would have an operating lifetime of at least twenty years. The basic scheme could also be extended to other structures at South Pole Station, such as the proposed shield for the South Pole Telescope. A photovoltaic system could be relatively easily implemented within the difficult environment of South Pole Station. It could also promote the adoption of other alternative energy solutions, such as wind turbines and regenerative fuel cell systems, within Antarctica. The underlying economic and environmental factors are conducive for the adoption of PV systems which would also demonstrate that the Antarctic research community is working to reduce the 'carbon cost' of their activities and to minimise their impact on this pristine environment.

References

1) US Antarctic Program
http://www.usap.gov

2) US building highway to the South Pole
www.newscientist.com 23 January 2003

3) Analysis of the Use of Wind Energy to Supplement the Power Needs at McMurdo Station and Amundsen-Scott South Pole Station Antarctica
Baring-Gould, R. Robichaud and K. McLain May 2005
National Renewable Energy Laboratory Technical Report NREL/TP-500-37504

4) US Defence Energy Support Centre
http://www.desc.dla.mil/default.asp

5) An Investigation into Fuel Utilisation and Energy Generation in Antarctica
Anna Mason GCAS Project Report 2006

6) Transportation; Research Platforms in Antarctica
http://quest.nasa.gov/antarctica/background/NSF/facts/fact03.html

7) U.S. Antarctic Program aircraft and supply ship operations, 2005-2006 season
www.nsf.gov/od/opp/antarct/treaty/usap_current/bigprint0506/bigprint_9.jsp

8) Key Pressures on the Ross Sea Region Environment (Antarctica NZ, 2001)

9) Testimony before the House Committee on Science Subcommittee on Basic Research
Dr Karl Erb June 9, 1999
http://www.nsf.gov/about/congress/106/kerb990609.jsp

10) Office of Polar Programs Advisory Committee
Report of the Subcommittee on U.S. Antarctic Program Resupply August 2005

11) South Pole Power Tiger Team Information
http://astro.uchicago.edu/scoara/2006-power/index.html

12) Scott Base Energy Audit – Event K424
January – April 2005 Main contributor: Dave Hume

13) NASA Surface Meteorology and Solar Energy
http://eosweb.larc.nasa.gov/sse

14) The History of PV
http://www.gosolar.u-net.com/complete_history_of_pv.htm

15) The Doping of Semiconductors
http://hyperphysics.phy-astr.gsu.edu/hbase/solids/dope.html#c3

16) The Physics of Solar Cells
J. Nelson Imperial College Press 2003 ISBN 1-86094-340-3

17) Photovoltaic Solar Energy Conversion
T. Markvart European Summer University: Energy for Europe, Strasbourg, 2002

18) Harnessing Solar Power
The Photovoltaics Challenge
K, Zweibel Plenum Press 1990 ISBN 0-306-43564-0

19) Underestanding Renewable Energy Systems
V. Quaschning Earthscan Publications 2005 ISBN 10-184-407128-6

20) Solar is Saving Energy for the Alfred A. Arraj U.S. Courthouse
Federal Energy Management Program Case Study
http://www1.eere.energy.gov/femp/pdfs/36633.pdf

21) Performance Monitoring of the Nunavut Arctic College PV System
Y. Poissant, D. Thevenard and D. Turcotte (paper based on article from SESCI 2004 conference)

22) Handbook of Photovoltaic Science and Engineering
A Luque and H. Hegedus John Wiley & Sons 2003

23) Renewable and Efficient Electric Power Systems
G. Masters Wiley Interscience 2004 ISBN 0-471-28060-7

24) Investigating the Effectiveness of Maximum Power Point Tracking for a Solar System
S. Armstrong and W. Hurley
IEEE Power Electronics Specialists Conference 2005

25) Thermal Environmental Engineering
T. H. Kuen, J. W. Ramsey and J. L. Threlkeld
Prentice Hall 1998 ISBN 10-013-917220-3

26) Photovoltaics in Cold Climates
M. Ross and J. Royer
James and James 1999 ISBN-1-873936 89-3

27) Solar Position Algorithm for Solar Radiation Application
Reda and Andreas 2003
NREL Technical Report NREL/TP-560-34302
available at www.osti.gov/bridge

28) Shell PowerMax Ultra 165-PC Product Information Sheet

29) Simple Test Methods for Evaluating the Energy Ratings of PV Modules under Various Environmental Conditions
Y. Poissant, L. Couture and L Dignard-Bailey

30) Solar Electric Power Generation – Photovoltaic Energy Systems
S. Krauter Springer 2006 ISBN-3-540-31345-1

31) Renewable Energy Sources
J. Twidell and T. Weir Taylor & Francis 2006 ISBN 0-419-25330-0

32) Designing with Solar Power
D. Prasad and M. Snow Images Publishing Group 2005 ISBN 1-876907-17-7